Open Access Publications by UMMS Authors

2020-04-15

Dbf4-Dependent Kinase (DDK)-Mediated Proteolysis of CENP-A Prevents Mislocalization of CENP-A in Saccharomyces cerevisiae

Jessica R. Eisenstatt
National Cancer Institute

Et al.

1 **Dbf4-Dependent Kinase (DDK)-Mediated Proteolysis of CENP-A Prevents Mislocalization**
2 **of CENP-A in *Saccharomyces cerevisiae***

3

4 Jessica R. Eisenstatt[*,1], Lars Boeckmann[*, 1, 2], Wei-Chun Au[*], Valerie Garcia[*], Levi Bursch[*],

5 Josefina Ocampo[†, 3], Michael Costanzo[‡, §], Michael Weinreich[**], Robert A. Sclafani[††], Anastasia

6 Baryshnikova[‡‡, 4], Chad L. Myers[§§], Charles Boone[‡, §], David J. Clark[†], Richard Baker[***], and

7 Munira A. Basrai[*]

8 [*]Genetics Branch, Center for Cancer Research, National Cancer Institute and [†]Division of

9 Developmental Biology, Eunice Kennedy Shriver National Institute for Child Health and Human

10 Development, National Institutes of Health, Bethesda, Maryland 20894, [‡]Department of

11 Molecular Genetics and [§]Donnelly Centre for Cellular and Biomolecular Research, Toronto,

12 Ontario M5S 3E1, Canada, [**]Van Andel Research Institute, 333 Bostwick Ave NE, Grand

13 Rapids, MI 49503, [††]Department of Biochemistry and Molecular Genetics, University of

14 Colorado School of Medicine, Aurora, Colorado 80045, [‡‡]Lewis-Sigler Institute for Integrative

15 Genomics, Princeton University, Princeton, New Jersey 08544, [§§]Department of Computer

16 Science and Engineering, University of Minnesota-Twin Cities, Minneapolis, Minnesota 55455,

17 and [***]Department of Microbiology and Physiological Systems, University of Massachusetts

18 Medical School, Worcester, Massachusetts 01655

19 [1]Authors contributed equally to this work.

20 [2]Present Address: University Medical Center Rostock, Clinic and Polyclinic for Dermatology

21 and Venerology, 18057 Rostock, Germany

22 [3]Present Address: Instituto de Investigaciones en Ingeniería Genética y Biología Molecular "Dr.

23 HéctorN. Torres" (INGEBI-CONICET), Buenos Aires, Argentina

24 [4]Present Address: Calico Life Sciences, South San Francisco, CA 94080, USA

25

26   Running title (35 characters): DDK prevents Cse4 mislocalization

27   Keywords (up to 5): Centromere, Cse4, CENP-A, DDK, Psh1, Cdc7

28   Corresponding Author: Munira A. Basrai, Genetics Branch, National Cancer Institute, National

29   Institutes of Health, 41 Medlars Drive, Rm B624, Bethesda, MD 20892. E-mail:

30   basraim@nih.gov Phone: 240-760-6746

31

32   **ABSTRACT**

33   The evolutionarily conserved centromeric histone H3 variant (Cse4 in budding yeast, CENP-A in

34   humans) is essential for faithful chromosome segregation. Mislocalization of CENP-A to non-

35   centromeric chromatin contributes to chromosomal instability (CIN) in yeast, fly, and human

36   cells and CENP-A is highly expressed and mislocalized in cancers. Defining mechanisms that

37   prevent mislocalization of CENP-A is an area of active investigation. Ubiquitin-mediated

38   proteolysis of overexpressed Cse4 (*GALCSE4*) by E3 ubiquitin ligases such as Psh1 prevents

39   mislocalization of Cse4, and *psh1Δ* strains display synthetic dosage lethality (SDL) with

40   *GALCSE4*. We previously performed a genome-wide screen and identified five alleles of *CDC7*

41   and *DBF4* that encode the Dbf4-dependent kinase (DDK) complex, which regulates DNA

42   replication initiation, among the top twelve hits that displayed SDL with *GALCSE4*. We

43   determined that *cdc7-7* strains exhibit defects in ubiquitin-mediated proteolysis of Cse4 and

44   show mislocalization of Cse4. Mutation of *MCM5* (*mcm5-bob1*) bypasses the requirement of

45   Cdc7 for replication initiation and rescues replication defects in a *cdc7-7* strain. We determined

46   that *mcm5-bob1* does not rescue the SDL and defects in proteolysis of *GALCSE4* in a *cdc7-7*

47   strain, suggesting a DNA replication-independent role for Cdc7 in Cse4 proteolysis. The SDL

48   phenotype, defects in ubiquitin-mediated proteolysis, and the mislocalization pattern of Cse4 in a

49   *cdc7-7 psh1Δ* strain were similar to that of *cdc7-7* and *psh1Δ* strains, suggesting that Cdc7

50   regulates Cse4 in a pathway that overlaps with Psh1. Our results define a DNA replication

51   initiation-independent role of DDK as a regulator of Psh1-mediated proteolysis of Cse4 to

52   prevent mislocalization of Cse4.

53

INTRODUCTION

55   The centromere, a specialized region of the chromosome that is essential for faithful

56 chromosome segregation, and associated proteins make up the kinetochore, which serves as an

57 attachment site for microtubules to promote segregation of sister chromatids during mitosis

58 (ALLSHIRE AND KARPEN 2008; VERDAASDONK AND BLOOM 2011; BURRACK AND BERMAN 2012;

59 CHOY *et al.* 2012; MADDOX *et al.* 2012; MCKINLEY AND CHEESEMAN 2016). Budding yeast

60 "point centromeres" consist of approximately 125 base pairs (bp) of unique DNA sequences,

61 whereas other eukaryotic organisms have "regional centromeres" consisting of several mega-bp

62 of repeated DNA sequences, satellite DNA arrays, or retrotransposon-derived sequences. Despite

63 the difference in the size of centromeres, the centromeric histone H3 variant (Cse4 in

64 *Saccharomyces cerevisiae*, Cnp1 in *Schizosaccharomyces pombe*, CID in *Drosophila*

65 *melanogaster*, and CENP-A in mammals) is evolutionarily conserved from yeast to human cells

66 and is essential for faithful chromosome segregation (PRZEWLOKA AND GLOVER 2009; CHOY *et*

67 *al.* 2012; HENIKOFF AND FURUYAMA 2012; BIGGINS 2013; WONG *et al.* 2020). Mislocalization of

68 overexpressed CENP-A and its homologs to non-centromeric regions contributes to

69 chromosomal instability (CIN) in yeast, fly, and human cells (HEUN *et al.* 2006; AU *et al.* 2008;

70 MISHRA *et al.* 2011; LACOSTE *et al.* 2014; ATHWAL *et al.* 2015; SHRESTHA *et al.* 2017). CIN and

71 high expression of CENP-A have been observed in cancer cells and this correlates with poor

72 prognosis and increased invasiveness (TOMONAGA *et al.* 2003; AMATO *et al.* 2009; LI *et al.*

73 2011; MCGOVERN *et al.* 2012; SUN *et al.* 2016; ZHANG *et al.* 2016). The mechanisms that

74 prevent the mislocalization of CENP-A and its homologs are not fully understood. Defining

75 these mechanisms will provide insight into how mislocalization of CENP-A contributes to

76 aneuploidy in human cancers.

77   Stringent regulation of cellular levels of Cse4 by post-translational modifications such as

78   ubiquitination prevents its mislocalization to non-centromeric regions in budding yeast, fission

79   yeast, and flies (COLLINS *et al.* 2004; MORENO-MORENO *et al.* 2006; MORENO-MORENO *et al.*

80   2011; AU *et al.* 2013; GONZALEZ *et al.* 2014). In addition to ubiquitination of Cse4, we have

81   recently defined a role for sumoylation in proteolysis of Cse4 (OHKUNI *et al.* 2016). Multiple

82   ubiquitin ligases, such as Psh1, Ubr1, the Sumo-targeted ubiquitin ligase Slx5, and the F-box

83   protein Rcy1 regulate proteolysis of overexpressed Cse4 (HEWAWASAM *et al.* 2010; RANJITKAR

84   *et al.* 2010; CHENG *et al.* 2016; OHKUNI *et al.* 2016; CHENG *et al.* 2017; OHKUNI *et al.* 2018).

85   Psh1 is one of the best characterized E3 ligases for proteolysis of overexpressed Cse4 and

86   prevents mislocalization of Cse4 to non-centromeric regions (HEWAWASAM *et al.* 2010;

87   RANJITKAR *et al.* 2010). Psh1 interacts with the CENP-A targeting domain (CATD) in the C-

88   terminus of Cse4 (HEWAWASAM *et al.* 2010; RANJITKAR *et al.* 2010) and mediates Cse4

89   degradation through the interaction of Psh1 with Spt16, a component of the FACT (facilitates

90   chromatin transcription) complex (DEYTER AND BIGGINS 2014). It has also been shown that

91   phosphorylation of Psh1 by casein kinase 2 (CK2) promotes degradation of Cse4 (HEWAWASAM

92   *et al.* 2014). In addition to targeting the C-terminus of Cse4, we have shown that the N-terminus

93   of Cse4 regulates Cse4 proteolysis (AU *et al.* 2013).

94   Mutant strains that show defects in Cse4 proteolysis display synthetic dosage lethality

95   (SDL) when Cse4 is overexpressed. However, Cse4 is not completely stabilized in *psh1Δ*, *ubr1Δ*,

96   *doa1Δ*, *slx5Δ*, or *rcy1Δ* strains (CHENG *et al.* 2017), suggesting the existence of additional

97   genes/pathways that regulate Cse4 proteolysis. We previously performed a Synthetic Genetic

98   Array (SGA) using conditional mutant alleles of essential genes to identify additional factors that

99   regulate Cse4 proteolysis (AU *et al.* 2020). The screen identified mutants encoding the F-box

100   proteins Met30 and Cdc4 of the Skp1, Cullin, F-box (SCF) complex. We defined a cooperative

101   role for Met30 and Cdc4 in the proteolysis of endogenous Cse4 to prevent its mislocalization and

102   promote chromosome stability (AU *et al.* 2020). Here, we pursued studies of the evolutionarily

103   conserved Dbf4-dependent kinase (DDK) complex as we identified five mutant *dbf4* and *cdc7*

104   alleles among the top twelve significant SDL hits. The DDK complex, which is essential for the

105   initiation of DNA replication, consists of the Cdc7 kinase and the regulatory subunit Dbf4

106   (JACKSON *et al.* 1993; STILLMAN 1996). DDK promotes the initiation of DNA replication by

107   phosphorylating Cdc45 and subunits of the mini-chromosome maintenance complex (Mcm2-7)

108   at origins of replication (LEI *et al.* 1997; OWENS *et al.* 1997; ZOU AND STILLMAN 2000; BRUCK

109   AND KAPLAN 2009). DDK also phosphorylates histone H3 at threonine 45 (H3T45) during S-

110   phase, which occurs in response to replication stress (BAKER *et al.* 2010), suggesting that H3T45

111   phosphorylation is linked with DNA replication. Previous studies have shown that centromeric

112   association of Cdc7 is important for early replication of centromeres (RAGHURAMAN *et al.* 2001;

113   ROSSBACH *et al.* 2017), which are among the earliest firing origins.

114   The identification of five *cdc7* and *dbf4* alleles that display SDL with overexpressed Cse4

115   led us to investigate the role of DDK in regulating Cse4 proteolysis. We determined that Cdc7

116   regulates Cse4 proteolysis in a pathway that overlaps with Psh1, and this prevents

117   mislocalization of Cse4. The role of Cdc7 in Cse4 proteolysis is independent of its role in the

118   initiation of DNA replication.

119

MATERIAL AND METHODS

121 **Strains and Plasmids**

122   Yeast strains were grown in YPD (1% yeast extract, 2% bacto-peptone, 2% glucose) or

123 synthetic medium with glucose or raffinose/galactose (2% final concentration each) and

124 supplements to allow for selection of the indicated plasmids. Yeast strains and plasmids used in

125 this study are described in Table S1 and Table S2, respectively. To integrate the *cdc7-7* allele

126 marked with the G418 resistance marker (KanMX), the *cdc7-7* sequence amplified from

127 RSY302 and the KanMX sequence were cloned into pGEM-T-Easy. *cdc7-7:KanMX* from the

128 vector was transformed into yeast strains as per standard lithium acetate procedure.

129 Transformants were screened for temperature sensitivity at 37°C and sequenced (CCR Genomics

130 Core) to confirm the G1137A mutation. Wild type *CDC7* marked with G418 resistance strains

131 were selected from the non-temperature sensitive transformants and sequenced to verify the wild

132 type *CDC7* sequence. To replace endogenous *CSE4* with HA-tagged *CSE4*, a PCR-based method

133 was used as described previously (BOECKMANN *et al.* 2013). Replacement of the *CSE4* gene with

134 HA-tagged *CSE4* was verified by sequencing and Western blots confirmed the expression of the

135 HA-tagged protein. At least two independent strains were analyzed for each experiment.

136

137 **Growth assays**

138   Wild type and mutant strains were transformed with the indicated plasmids or the empty

139 vector. Transformants grown on synthetic medium, selective for the plasmid, were suspended in

140 water to a concentration with an optical density of 1 measured at a wavelength of 600 nm

141 (OD_{600}, approximately 1.0×10^7 cells per ml). Five-fold serial dilutions starting with 1 OD_{600}

142 were generated and 3 μl of each dilution spotted on synthetic growth medium selecting for the

143 plasmid and containing either glucose (2% final concentration) or galactose and raffinose (2%

144 final concentration each). Strains were grown at the indicated temperatures for 3-5 days. Three

145 independent transformants were assayed for growth unless otherwise stated.

146

147 **Protein stability assays**

148   Protein stability assays were performed as previously described (Au *et al.* 2008). Briefly,

149 strains were grown to logarithmic phase overnight in selective media, re-suspended in fresh

150 media containing galactose/raffinose (2% final concentration each) and grown for 1.75 or four

151 hours as indicated in figure legends at 23°C. 10 µg/ml cycloheximide (CHX) and glucose (2%

152 final concentration) were added to cultures and aliquots were collected 0, 30, 60, 90, and 120

153 minutes after CHX addition. Proteins were isolated using the TCA method as described

154 previously (Kastenmayer *et al.* 2006). Protein levels were standardized using the Bio-Rad

155 DC™ Protein Assay. Samples were diluted 1:1 with Laemmli buffer containing BME and stored

156 at -20°C for Western blot analysis. Proteins were separated by SDS-PAGE on 4-12% Bis-TRIS

157 SDS-polyacrylamide gels (Novex, NP0322BOX). Western blot analysis was done using primary

158 antibodies α-HA (1:1000, Roche, 12CA5), α-Flag (1:5000, Sigma, F3165), or α-Tub2 (1:4500,

159 custom made for Basrai Laboratory) in TBST containing 5% (w/v) dried skim milk. HRP-

160 conjugated sheep α-mouse IgG (Amersham Biosciences, NA931V) and HRP-conjugated donkey

161 α-rabbit IgG (Amersham Biosciences, NA934V) were used as secondary antibodies. Blots were

162 washed after primary and secondary antibodies with TBST (Tris-buffered saline plus 0.1%

163 Tween 20) three times for 10 minutes. Western blots were quantified with the SynGene program

164 (SynGene, Cambridge, UK) or the Image Lab Software (BioRad). Protein stability of Cse4 was

165 measured as the percent remaining after normalization to Tub2 signal.

166

Ubiquitination (Ub) Pull-down Assay

167

168　　　Ub pull-down assays for determining the levels of ubiquitinated Cse4 were performed as

169　described previously (Au *et al.* 2013) with minor modifications. Strains were grown to

170　logarithmic phase overnight in selective media, re-suspended in fresh media containing

171　galactose/raffinose (2% final concentration each) and grown for four hours at 23°C. Cells were

172　resuspended in Cell Lysis Buffer with freshly added protease inhibitor cocktail, PMSF, and

173　NEM (inhibitor for de-ubiquitination) and lysed by vortexing for 1 hour at 4°C in the presence of

174　glass beads. The concentration of proteins in each resulting lysate was measured and normalized.

175　50 µl lysate was saved for input and the remaining lysate was added to Tandem Ubiquitin

176　Binding Entity (TUBE) beads (LifeSensors) and incubated overnight at 4ºC. Beads were

177　centrifuged and washed three times with TBST on a rocking platform; unbound lysate was

178　collected. Beads were resuspended in Laemmli buffer and incubated for 10 minutes at 100°C.

179　Input and unbound fraction containing Laemmli buffer were processed in parallel. Samples were

180　analyzed using Western Blot. Western blots were quantified with the SynGene program

181　(SynGene, Cambridge, UK). *p*-value was determined using a paired t-test (GraphPad Prism).

182

Chromosome spreads

183

184　　　Chromosome spreads were performed as previously described (Collins *et al.* 2004;

185　Crotti and Basrai 2004; Collins *et al.* 2007) with minor modifications. Cultures were grown

186　to logarithmic phase in selective medium containing 2% raffinose and treated with Nocodazole

187　(20 µg/ mL final) for three hours to arrest cells in the G2/M phase of the cell cycle. FACS

188　analysis confirmed the cell cycle arrest. For the last hour of the Nocodazole arrest, galactose was

189　added to 2% final concentration. Cells were lysed gently by treatment with zymolase-100T and

190　BME. Spheroplasts were then spread onto glass slides and fixed with paraformaldehyde and 1%

191   lipsol and allowed to air dry. Slides were washed with 1 X PBS for 10 minutes and incubated in

192   16B12 Mouse anti-HA primary antibody (1:2500). Slides were washed three times with 1 X PBS

193   for 10 min and incubated with Cy3 conjugated Goat anti-mouse secondary antibody (1:5000).

194   Slides were washed with 1 X PBS and mounted with antifade containing DAPI and visualized

195   using DeltaVision Microscopy Imaging Systems. Nuclei with a single or two HA- or Flag-Cse4

196   foci were counted as normal Cse4 localization and nuclei with multiple foci or a diffused signal

197   in the nucleus were counted as mislocalized Cse4. At least 360 cells were counted for each

198   experiment. *p*-values were determined using Ordinary one-way ANOVA (GraphPad Prism)

199

200   **ChIP-Seq**

201   Chromatin immunoprecipitations were performed as previously described (COLE *et al.*

202   2014; CHEREJI *et al.* 2017) with modifications. Cultures grown to logarithmic phase in glucose or

203   raffinose/galactose media for 1.75 hours were treated with formaldehyde (final 1%) for 20

204   minutes at 30°C followed by the addition of 2.5 M glycine for 10 minutes. Cells were washed

205   twice with 1 X PBS and resuspended in 2 mL FA Lysis Buffer (1 mM EDTA pH8.0, 50 mM

206   HEPES-KOH pH7.5, 140 mM NaCl, 0.1% sodium deoxycholate, 1% Triton X-100) with 1 x

207   protease inhibitors (Sigma) and 1 mM PMSF final concentration. The cell suspension was split

208   into four screw top tubes with glass beads (0.4-0.65 mm diameter) and lysed three times for 40

209   seconds each, followed by a five-minute rest on ice, and lysed two times for 40 seconds each in

210   an MP Bio FastPrep-24 5G. The cell lysate was collected, and the chromatin pellet was washed

211   twice in FA Lysis Buffer. Each pellet was resuspended in 600 µl of FA Lysis Buffer and

212   combined into one 5 ml tube. The chromatin suspension was sonicated 24 times with repeated 15

213   seconds on/off at 20% amplitude using a Branson digital sonifer. After 3 minutes of

214   centrifugation (13000 rpm, 4°C), the supernatant was transferred to another tube. About 5% was

215   used for input and checking the size of sheared DNA. The remaining was incubated with 150 µl

216   anti-FLAG® M2 Affinity Gel (Sigma, A2220-5ML) overnight. The beads were washed for five

217   minutes on a rotator in 1 ml FA, FA-HS (500 mM NaCl), RIPA, and TE buffers twice each. The

218   beads were resuspended in ChIP Elution Buffer (25 mM Tris-HCl pH7.6, 100 mMNaCl, 0.5%

219   SDS) and incubated at 65°C overnight. The beads were treated with proteinase K (0.5 mg/ml) at

220   55°C for four hours followed by Phenol/Chloroform extraction and ethanol precipitation. The

221   DNA pellet was resuspended in a total of 50 µl sterile water.

222   Input and IP samples were repaired using the NEB Pre-PCR Repair Mix (New England

223   Biolabs, M0309). Paired-end libraries for input and IP samples were prepared using the

224   NEBNext® End Prep (New England Biolabs, E7370) and NEBNext® Multiplex Oligos for

225   Illumina (New England Biolabs, E7335). Agencourt AMPure XP beads (Beckman-Coulter,

226   A63880) were used to purify adaptor-ligated DNA samples and PCR products (input adapters

227   diluted 1/3 and IP 1/250). The 50-base paired-end Illumina reads were aligned to the *S.*

228   *cerevisiae* S288C reference (R64-2-1) using Bowtie version 1.0.0 with command line options -n2

229   -m1 -X 500. Duplicate reads (20-89%) were removed using Samtools rmdup (version 0.1.19).

230   Between 1.4M and 5.3M unique alignments remained for the ChIP libraries and 14M-24M for

231   the input libraries. The input alignments were randomly down sampled to 10M alignments each.

232   Peaks were called using MACS (ZHANG *et al.* 2008) version 2.1.1.20160226 in paired-end mode

233   with default parameters and no additional down sampling.

234   The annotatePeaks tool of the Hypergeometric Optimization of Motif EnRichment suite

235   (HOMER v5.10; http://homer.ucsd.edu/homer/) was used to assign peaks of Cse4 enrichment to

236   genomic features. Customized annotations were utilized. Similar to the approach of Hildebrand

237   and Biggins (HILDEBRAND AND BIGGINS 2016), 5'- and 3'-UTR's were annotated using the data

238   of Nagalakshmi *et al.* (NAGALAKSHMI *et al.* 2008) downloaded from the yeast genome browser

239   (https://browse.yeastgenome.org). 5'- and 3'-prime UTR data was available for 4605 and 5175

240   genes, respectively. For genes lacking UTR data, UTR's were assigned a median length (53 and

241   105 nucleotides, respectively). Promoters were defined as the region lying 500 bp upstream of

242   the transcription start site (i.e., position 1 of the 5'-UTR). Transcription termination sites were

243   defined as ± 50 bp from the end of the 3'-UTR.

244   Intersections between peak sets were computed using the IntersectRegions function of the

245   USeq suite (http://useq.sourceforge.net) which also provides an estimate of statistical

246   significance by randomization of one of the target peak sets across the genome. Coverage tracks

247   were computed by MACS and normalized to 1M reads and displayed using the Integrative

248   Genomics Viewer (ROBINSON *et al.* 2011).

249

250   **Data availability**

251   Strains and plasmids are available upon request. Supplemental file S1 contains Table S1, which

252   describes the strains used in this study, and Table S2, which lists the plasmids used. Figures S1,

253   S2, and S3 are available as supplemental files. Supplemental files are available at FigShare.

254   ChIP-seq data for wild type and *cdc7-7* strains with *Flag-Cse4* expressed from its own promoter

255   and *GAL-Flag-Cse4* integrated into the genome are available at GEO with accession number

256   GSE148068.

257

RESULTS

259 **Mutants of the Cdc7-Dbf4 kinase complex exhibit SDL with *GALCSE4***

260   To identify mutants of essential genes that display synthetic dosage lethality (SDL) when

261 Cse4 is overexpressed (*GALCSE4*), we performed a Synthetic Genetic Array (SGA) (AU *et al.*

262 2020). A strain in which *GAL-HA-CSE4* was integrated in the genome was mated to an array of

263 786 conditional temperature sensitive strains. Growth at 26°C of the haploid meiotic progeny

264 was scored on galactose plates and the *p*-value was determined as previously described

265 (BARYSHNIKOVA *et al.* 2010; COSTANZO *et al.* 2010; COSTANZO *et al.* 2016). Among the top

266 twelve hits that show SDL are five alleles of genes encoding the Dbf4-dependent kinase (DDK)

267 complex, the gene encoding calmodulin, and regulators of proteasome assembly, mRNA

268 polyadenylation, and cell cycle progression (Table 1). The identification of multiple alleles

269 encoding components of the DDK complex led us to further investigate a possible role of DDK

270 in regulating cellular levels of Cse4 to prevent mislocalization of Cse4 to non-centromeric

271 regions. We confirmed the SDL phenotype using growth assays in which yeast strains

272 transformed with a plasmid containing *GALCSE4* or empty vector (vector) were plated on media

273 with glucose or galactose to induce expression of *GALCSE4*. Strains with mutations in either

274 *CDC7* (Figure 1A; *cdc7-4*) or *DBF4* (Figure 1A; *dbf4-1, dbf4-2*) exhibited *GALCSE4* SDL at the

275 permissive temperature of 23°C on galactose media. A *cdc7-7* mutant, which was not included in

276 the SGA screen, also exhibited *GALCSE4* SDL (Figure 1A). We pursued in-depth studies with

277 the *cdc7-7* mutant because the *cdc7-7* allele displays a stronger SDL phenotype at 23°C, has a

278 low frequency of induced mutagenesis, does not have defects in the cell cycle at 23°C, and

279 exhibits DNA replication defects only at the non-permissive temperature of 37°C

280 (HOLLINGSWORTH JR *et al.* 1992). To establish that the SDL phenotype of a *cdc7-7 GALCSE4*

281 strain is linked to the *CDC7* gene, we performed growth assays with *cdc7-7 GALCSE4* strains

282   with plasmid-borne *CDC7* or empty vector. The plasmid-borne *CDC7* rescued the temperature

283   sensitivity of the *cdc7-7* strain at 37°C and the SDL phenotype of *cdc7-7 GALCSE4* at 23°C

284   (Figure 1B).

285   **Cdc7 regulates ubiquitin-mediated proteolysis of Cse4**

286   Previous studies have shown that defects in ubiquitin-mediated proteolysis of

287   overexpressed Cse4 contribute to *GALCSE4* SDL in *psh1Δ*, *slx5Δ,* and *hir2Δ* strains

288   (HEWAWASAM *et al.* 2010; RANJITKAR *et al.* 2010; OHKUNI *et al.* 2016; CIFTCI-YILMAZ *et al.*

289   2018). The SDL phenotype of DDK mutants led us to hypothesize that proteolysis of Cse4 is

290   regulated by the DDK complex. Therefore, we examined the stability of overexpressed HA-Cse4

291   in wild type, *cdc7-7*, and *dbf4-1* strains after treatment with cycloheximide at 23°C. Increased

292   stability of HA-Cse4 was observed in *cdc7-7* (Figure 2A) and *dbf4-1* (Figure 2B) strains when

293   compared to that in a wild type strain.

294   It has been shown that defects in ubiquitination of Cse4 contribute to increased protein

295   stability and mislocalization of Cse4 in a *psh1Δ* strain (HEWAWASAM *et al.* 2010; RANJITKAR *et*

296   *al.* 2010). The increased stability of Cse4 led us to examine if a *cdc7-7* strain exhibits defects in

297   poly-ubiquitination of overexpressed HA-Cse4 (Ub_n-Cse4). We performed an affinity pull-down

298   of ubiquitinated proteins and consistent with previous studies (AU *et al.* 2013), we detected

299   ubiquitinated Cse4 as a laddering pattern in wild type cells (Figure 2C). Quantification of signal

300   intensities of Ub_n-Cse4 normalized to signal intensities of Cse4 in input samples showed a

301   significant reduction in the levels of ubiquitinated Cse4 in a *cdc7-7* strain compared to a wild

302   type strain (Figure 2C, *p*-value < 0.05). The defects in Cse4 proteolysis and Cse4 ubiquitination

303   in the *cdc7-7* strains suggest that Cdc7 regulates ubiquitin-mediated proteolysis of Cse4.

Cdc7 regulates proteolysis of Cse4 independently of its role in DNA replication initiation

304

305   Previous studies have shown that DDK activates the initiation of DNA replication

306   through phosphorylation of the MCM2-7 complex (LEI *et al.* 1997; OSHIRO *et al.* 1999;

307   WEINREICH AND STILLMAN 1999; ZOU AND STILLMAN 2000; BRUCK AND KAPLAN 2009). DNA

308   replication defects are observed in *cdc7* strains at the non-permissive temperature of 37°C

309   (SCLAFANI 2000), but DNA replication is unperturbed in *cdc7-7* strains grown at 23°C (JACKSON

310   *et al.* 1993). Mutation of proline 83 of *MCM5* to leucine (*mcm5-bob1*) bypasses specifically the

311   requirement of Cdc7 for replication initiation and rescues the temperature sensitivity and

312   replication defects of *cdc7-1* and *cdc7-7* strains at 37°C (HARDY *et al.* 1997; SCLAFANI *et al.*

313   2002; HOANG *et al.* 2007). We observed the *GALCSE4* SDL phenotype and stability of HA-Cse4

314   in *cdc7-7* strains at 23°C. To further confirm that Cdc7-mediated proteolysis of Cse4 is

315   independent of its role in initiating DNA replication, we performed growth assays for the SDL

316   phenotype with the *cdc7-7 mcm5-bob1* double mutant with *GALCSE4*. Our results showed that

317   the *cdc7-7 mcm5-bob1 GALCSE4* strain exhibited SDL similar to that observed in the *cdc7-7*

318   *GALCSE4* strain at 23°C (Figure 3A). Next, we determined if the *mcm5-bob1* mutation affects

319   the proteolysis of overexpressed HA-CSE4 in a *cdc7-7* strain. Protein stability assays were done

320   with extracts from wild type, *cdc7-7*, *mcm5-bob1*, and *cdc7-7 mcm5-bob1* strains expressing

321   *GAL-HA-CSE4*. The stability of HA-Cse4 in the *mcm5-bob1* strain was similar to that of the wild

322   type strain (Figure 3B). Furthermore, the defects in proteolysis of HA-Cse4 observed in the

323   *cdc7-7* strain were not suppressed in the *cdc-7 mcm5-bob1* strain (Figure 3B). The inability of

324   the *mcm5-bob1* mutation to rescue the SDL phenotype and proteolysis defect in a *cdc7-7*

325   *GALCSE4* strain suggests that the role of Cdc7 in regulating Cse4 proteolysis is independent of

326   Cdc7's role in initiating DNA replication.

Cse4 is mislocalized to non-centromeric regions with an enrichment at promoters in a *cdc7-7* strain

We next examined the localization pattern of Cse4 using chromosome spreads, a method that eliminates soluble material to visualize chromatin-bound HA-Cse4 in WT and *cdc7-7* strains. Previous studies have shown that Cse4 is localized to kinetochores that are clustered in one or two discrete nuclear foci in wild type cells, whereas mislocalization of Cse4 shows more than two foci or diffuse signal through the nuclear mass in *psh1Δ*, *slx5Δ*, and *hir2Δ* strains (HEWAWASAM *et al.* 2010; RANJITKAR *et al.* 2010; OHKUNI *et al.* 2016; CIFTCI-YILMAZ *et al.* 2018). In the *cdc7-7* strain, we found that, in contrast to wild type cells, HA-Cse4 was mislocalized with signal at more than two foci or diffused across the nuclear mass (Figure 4A and 4B, *cdc7-7*, *p*-value = 0.0028). To determine if the mislocalization of HA-Cse4 in a *cdc7-7* strain is due to a kinetochore clustering defect, we examined the localization of the kinetochore protein Mtw1-GFP (PINSKY *et al.* 2003; WESTERMANN *et al.* 2003). Our results showed a similar localization pattern of Mtw1-GFP to one or two foci in both the wild type (97.5%) and *cdc7-7* (94.6%) cells (Figure 4C and 4D). This suggests that the mislocalization of HA-Cse4 in a *cdc7-7* mutant is not due to kinetochore de-clustering. Based on these results, we conclude that DDK regulates ubiquitin-mediated proteolysis of Cse4 and prevents mislocalization of Cse4 to non-centromeric regions.

We next performed ChIP-seq experiments to define the genome-wide localization pattern of endogenous and overexpressed Cse4 in a *cdc7-7* strain. ChIP-seq was performed using chromatin from wild type and *cdc7-7* strains with endogenous Flag-Cse4 expressed from its own promoter grown at 23°C in glucose or with galactose-inducible Flag-Cse4 integrated in the genome and grown at 23°C in galactose media for 1.75 hours to overexpress Flag-Cse4. Consistent with previous reports (HILDEBRAND AND BIGGINS 2016), endogenous Flag-Cse4

351   showed peaks of enrichment primarily at centromeric (*CEN*) regions in the wild type strain

352   (Figure S1, WT). Endogenous Flag-Cse4 also showed enrichment primarily at *CEN* regions in

353   the *cdc7-7* strain (Figure S1, *cdc7-7*), indicating that Flag-Cse4 expressed from its own promoter

354   is not mislocalized to distinct non-centromeric genomic loci in a *cdc7-7* strain. For

355   overexpressed Flag-Cse4, at the sequencing depth of our experiments (1.5-5.3 million non-

356   duplicates, uniquely-mapped reads), Flag-Cse4 was found enriched at only 30 non-*CEN* sites in a

357   wild type strain. In contrast, 2,187 non-*CEN* peaks of Flag-Cse4 were detected in a *cdc7-7 GAL-*

358   *FLAG-CSE4* strain. In addition, a higher generalized background of Flag-Cse4 was observed

359   across the genome as evidenced by a lower signal to noise ratio of the *CEN* peaks (Figure 5A,

360   S2). Our results show that overexpressed Flag-Cse4 is highly enriched at promoters (60.4% of

361   total peaks and 2.75-fold enriched relative to feature target size), but not at 3'-UTR's,

362   transcription termination sites (TTS), exons, introns, and intergenic regions in the *cdc7-7* strain

363   (Figure 5B). Significant enrichment (3.1-fold) was also found at 5'-UTR's, although only 9.8%

364   of the total peaks were found at these locations. This result is likely attributable to peaks

365   overlapping the boundary between promoter and 5'-UTR.

366   The phenotypes of SDL with *GALCSE4*, defects in Cse4 proteolysis, and mislocalization

367   of Cse4 to non-centromeric regions in a *cdc7-7* strain are similar to that observed in a *psh1Δ*

368   strain (HEWAWASAM *et al.* 2010; RANJITKAR *et al.* 2010). Since the ChIP-seq experiments were

369   performed with an isogenic set of strains with an integrated copy of *GAL-FLAG-CSE4* in the

370   same genetic background used previously to examine localization of overexpressed Flag-Cse4 in

371   a *psh1Δ* background (HILDEBRAND AND BIGGINS 2016), we compared our results to the ChIP-seq

372   results from Hildebrand and Biggins. The raw sequencing data was downloaded from the

373   Sequence Read Archive (GEO Series GSE69696) and subjected to the same alignment and peak

374   calling procedures used for our ChIP-seq analyses with the *cdc7-7* strain. Of the 2,129 regions of

375   Flag-Cse4 enrichment identified in the *cdc7-7* strain 2,059 (97%) overlapped with one or more

376   peaks of Cse4 enrichment identified in the *psh1Δ* strain (p-value $< 10^{-4}$) (Figure 5C). As

377   observed for the *psh1Δ* strain, a high proportion (1,994/2,129, 94%) of Cse4 mislocalization in

378   the *cdc7-7* strain occurs in promoter regions (p-value $< 10^{-4}$); virtually all were common to

379   promoter-localized Cse4 found in the *psh1Δ* strain (Figure 5C). We note that in making the 3-

380   way comparison, closely-spaced peaks are merged to eliminate inconsistency in counts when a

381   single peak in one set overlaps multiple peaks in another set; thus, the total number of intervals

382   shown in Figure 5C differs from the actual *cdc7-7* peak count indicated in Figure 5B. Overall,

383   these results show that the mislocalization pattern of Cse4 in the *cdc7-7* strain is similar to that

384   observed in a *psh1Δ* strain.

385   **Cdc7 regulates Psh1-mediated proteolysis of overexpressed Cse4**

386   We have previously shown that overexpression of the ubiquitin-encoding gene *UBI4*

387   suppresses the SDL of a *psh1Δ GALCSE4* strain (AU *et al.* 2013). The overlapping pattern of

388   Cse4 mislocalization in *cdc7-7* and *psh1Δ* strains prompted us to examine if overexpression of

389   *UBI4* would suppress the SDL of a *cdc7-7 GALCSE4* strain. Growth assays showed that *UBI4*

390   suppresses the *cdc7-7 GALCSE4* SDL phenotype at the permissive temperature of 23°C (Figure

391   6A). *UBI4* did not suppress the TS growth defect of *cdc7-7* strains at 37°C.

392   We took multiple approaches to evaluate if Cdc7 functions in an overlapping pathway

393   with Psh1 to regulate Cse4 proteolysis. We generated *cdc7-7* and *psh1Δ* single and *cdc7-7 psh1Δ*

394   double mutant strains with *GAL-FLAG-CSE4* integrated in the genome. Growth assays

395   confirmed the SDL phenotype of *GAL-FLAG-CSE4* for *cdc7-7* (Figure 1A and 6B), and that

396   reported previously for *psh1Δ* strains on galactose media (HEWAWASAM *et al.* 2010; RANJITKAR

397   *et al.* 2010). The *psh1Δ* strain showed a more severe growth defect than the *cdc7-7* strain with

398   *GAL-FLAG-CSE4*. The *cdc7-7 psh1Δ* double mutant displays SDL similar to that observed for

399   the *psh1Δ* strain (Figure 6B). We also examined the stability of overexpressed Flag-Cse4 in the

400   *cdc7-7*, *psh1Δ*, and *cdc7-7 psh1Δ* strains. Consistent with previous results (Figure 2A and

401   (HEWAWASAM *et al.* 2010; RANJITKAR *et al.* 2010)), Flag-Cse4 was more stable in *cdc7-7* and

402   *psh1Δ* strains when compared to the wild type strain (Figure 6C). The stability of Flag-Cse4 in

403   the *psh1Δ* strain is higher than that in the *cdc7-7* strain, however the stability of Flag-Cse4 in the

404   *cdc7-7 psh1Δ* strain was similar to that observed in the *psh1Δ* strain (Figure 6C). Lastly, we

405   examined the mislocalization of Flag-Cse4 in wild type, *cdc7-7*, *psh1Δ*, and *cdc7-7 psh1Δ* strains

406   using chromosome spreads. We observed significantly higher levels of Flag-Cse4

407   mislocalization in *cdc7-7* as described earlier (Figures 4A and 4B) and as reported previously for

408   *psh1Δ* strains (HEWAWASAM *et al.* 2010; RANJITKAR *et al.* 2010) when compared to the wild

409   type strain. Consistent with results for the SDL phenotype and protein stability, the

410   mislocalization of Flag-Cse4 was not further enhanced in *cdc7-7 psh1Δ* strains when compared

411   to the single *cdc7-7* and *psh1Δ* strains (Figure 6D, *p*-value > 0.999). We propose that Cdc7 and

412   Psh1 are epistatic for proteolysis of Cse4 to prevent Cse4 mislocalization to non-centromeric

413   regions.

414

DISCUSSION

415

416   In this study, we investigated the role of the Dbf4-dependent kinase (DDK) complex in

417   proteolysis of Cse4. Five alleles of genes encoding DDK were among the top twelve hits in a

418   screen to identify mutant strains displaying SDL with *GALCSE4*. Our results show that *cdc7-7*

419   strains exhibit an SDL phenotype with *GALCSE4,* defects in ubiquitin-mediated proteolysis of

420   Cse4, and mislocalization of Cse4 to non-centromeric regions, particularly to gene promoters.

421   The lack of a rescue of the *GALCSE4 SDL* or Cse4 proteolysis defect in the *cdc7-7* strain by

422   *mcm5-bob1* indicates a DNA replication-independent role of Cdc7 in Cse4 proteolysis.

423   Additionally, several experimental approaches showed that Cdc7 functions in a pathway

424   overlapping with Psh1 to promote proteolysis of Cse4 and prevent Cse4 mislocalization to non-

425   centromeric regions. Our studies define the first essential kinase, DDK, to regulate proteolysis of

426   overexpressed Cse4 and prevent mislocalization of Cse4.

427   DDK is most well-studied for its role in initiating DNA replication through

428   phosphorylation of the MCM2-7 DNA helicase complex at origins of replication, allowing cells

429   to proceed through the G1/S phase of the cell cycle (LEI *et al.* 1997; OSHIRO *et al.* 1999;

430   WEINREICH AND STILLMAN 1999; ZOU AND STILLMAN 2000; BRUCK AND KAPLAN 2009).

431   Temperature sensitive *cdc7* mutants exhibit defects in the cell cycle and are unable to complete

432   DNA replication at the restrictive temperature of 37°C; replication and cell cycle defects are not

433   observed at the permissive temperature of 23°C (reviewed in (SCLAFANI 2000)). All the assays in

434   our current study, including growth, protein stability, and chromosome localization, were

435   performed at 23°C. Based on these results, we conclude that the *GALCSE4* SDL phenotype,

436   defect in Cse4 proteolysis, and decrease in Ub_n-Cse4 levels in *cdc7-7* strains observed at 23°C

437   are independent of defects in cell cycle progression.

438   Phosphorylation of MCM2-7 by DDK causes a conformational change in the MCM2-7

439   complex and this regulates replication initiation (HOANG *et al.* 2007). A mutation in MCM5,

440   P83L (*mcm5-bob1*), is thought to mimic the conformational change that results from DDK-

441   mediated phosphorylation of MCM2-7. The *mcm5-bob1* mutation rescues the temperature

442   sensitivity, bypasses the cell cycle defects of *cdc7* strains (JACKSON *et al.* 1993), and the DNA

443   distribution by FACS of a *cdc7 mcm5-bob1* strain is normal (HARDY *et al.* 1997). We used

444   genetic and biochemical approaches to examine if the role of Cdc7 in proteolysis of Cse4 is

445   independent of its role in replication initiation. We reasoned that if the regulation of Cse4

446   proteolysis by Cdc7 was dependent on replication initiation, the *mcm5-bob1* mutation should

447   rescue the SDL phenotype and Cse4 proteolysis defect in *cdc7-7* strains. However, we did not

448   observe suppression of the *GALCSE4* SDL or defects in Cse4 proteolysis in the *cdc7-7 mcm5-*

449   *bob1* strain at 23°C. Furthermore, ChIP-seq using a *cdc7-7* strain did not reveal a significant

450   enrichment of Cse4 to origins of DNA replication which are normally occupied by Cdc7

451   (ROSSBACH *et al.* 2017). Similar to our observations, a previous study has shown that *mcm5-*

452   *bob1* cannot suppress the defect of *cdc7*-induced mutagenesis (PESSOA-BRANDAO AND SCLAFANI

453   2004), indicating a different Cdc7 substrate in mutagenesis than the MCM2-7 complex

454   (ROSSBACH AND SCLAFANI 2016). Together, our results support a DNA replication-independent

455   role of Cdc7 in regulating Cse4 proteolysis.

456   Cse4 expressed from its own promoter is not detectably mislocalized to specific genomic

457   regions in a *cdc7-7* strain (Figure S1). Additionally, degradation of endogenous Flag-Cse4 in a

458   *cdc7-7* strain is similar to that in a wild type strain (Figure S3). Genome-wide studies have

459   shown that mislocalization of Cse4 is barely detectable in wild type (CAMAHORT *et al.* 2009;

460   LEFRANCOIS *et al.* 2009; HILDEBRAND AND BIGGINS 2016) or *psh1Δ* strains (HILDEBRAND AND

461 BIGGINS 2016), suggesting that cellular levels of endogenous Cse4 are stringently regulated to

462 ensure that it is not mislocalized to non-centromeric regions in a wild type cell. In the context of

463 overexpressed Cse4, wild type cells do not show growth inhibition with *GAL-CSE4*, in part

464 because overexpressed Cse4 is proteolyzed by Psh1, Rcy1, Slx5, Ubr1, and other regulators.

465 Mutants of these regulators display defects in proteolysis of Cse4, which contributes to

466 mislocalization of overexpressed Cse4 and lethality with *GAL-CSE4* (HEWAWASAM *et al.* 2010;

467 RANJITKAR *et al.* 2010; OHKUNI *et al.* 2016; CIFTCI-YILMAZ *et al.* 2018).

468   Our studies here provide evidence that Cdc7 plays a role in regulating levels of

469 overexpressed Cse4. Chromosome spreads showed mislocalization of overexpressed Cse4 in a

470 *cdc7-7* strain and ChIP-seq confirmed these results. We observed a significant amount of Cse4

471 mislocalization throughout the genome, and analysis of the localization pattern showed a

472 preferential enrichment of Flag-Cse4 at promoter regions with a high degree of overlap to that

473 observed in the *psh1Δ* strain. We propose that Cdc7 functions in a pathway that overlaps with

474 Psh1 in Cse4 proteolysis. We provide several lines of evidence to support our hypothesis. The

475 *GALCSE4* SDL phenotype, increased stability of Cse4, and levels of Cse4 mislocalization

476 observed in the *cdc7-7 psh1Δ* strain were not significantly different than that observed in the

477 *cdc7-7* or *psh1Δ* strains. Additionally, the preferential localization of Cse4 to promoters is

478 observed in both *cdc7-7* and *psh1Δ* strains and the *GALCSE4* SDL phenotype is suppressed by

479 overexpression of *UBI4* in both *cdc7-7* and *psh1Δ* strains. Future studies will allow us to

480 investigate the mechanism by which Cdc7 affects the Psh1 pathway and if Cdc7 regulates

481 pathways other than Psh1-mediated proteolysis for Cse4.

482   Previous studies have shown that Cdc7 and Dbf4 associate with replication origins,

483 including the early-firing replication origins at the centromere (NATSUME *et al.* 2013; ROSSBACH

484 *et al.* 2017) and that low levels of DDK at centromeres contributes to delay in the replication of

485 centromeres (NATSUME *et al.* 2013). DDK associates with kinetochores through the COMA

486 complex, consisting of Ctf19, Mcm21, Okp1, and Ame1, and this regulates sister chromatid

487 cohesion independently of the role of DDK in initiating DNA replication (NATSUME *et al.* 2013).

488 DDK phosphorylates the N-terminal tail of Ctf19 and this recruits the cohesin loader Scc2/4, for

489 proper sister chromatid cohesion (HINSHAW *et al.* 2017). Recent studies have shown that the N-

490 terminal tail of Cse4 interacts with Okp1, which directs kinetochore loading distinct from Mif2-

491 directed loading (FISCHBÖCK-HALWACHS *et al.* 2019). Phosphorylation of the N-terminal tail of

492 Cse4 promotes the interaction of Cse4 with Ame1/Okp1 and this likely regulates recruitment of

493 kinetochore components (HINSHAW AND HARRISON 2019). It is of great interest to examine if

494 Cse4 is a substrate of DDK and define the role of DDK-mediated phosphorylation of Ctf19 for

495 the association of the COMA complex with Cse4. Future studies will allow us to examine if

496 DDK-mediated phosphorylation of kinetochore substrates such as Cse4, Psh1, and Ctf19

497 contribute to the proteolysis of overexpressed Cse4 and prevent its mislocalization to non-

498 centromeric regions.

499   In this study, we have described a new role for the essential kinase Cdc7 in regulating

500 Psh1-mediated proteolysis of Cse4 independently of Cdc7's role in initiating DNA replication.

501 Based on our results for SDL of *GALCSE4* in *cdc7-7* strains, we propose that inhibition of Cdc7

502 in cancers with high levels of CENP-A would lead to cancer cell-specific cell death. These

503 studies are relevant from a clinical standpoint because high levels of Cdc7 and Dbf4 expression

504 have been reported in several types of cancers (BONTE *et al.* 2008) and this correlates with

505 accelerated progression through the cell cycle, mutation of p53, resistance to DNA damaging

506 agents and chemotherapy, and poor survival rates (MONTAGNOLI *et al.* 2004; BONTE *et al.* 2008;

507   KULKARNI *et al.* 2009; RODRIGUEZ-ACEBES *et al.* 2010; HOU *et al.* 2012; CHENG *et al.* 2013).

508   Targeting Cdc7 through siRNA knockdown in cancer cells has been shown to result in cancer

509   cell-specific apoptotic cell death (BONTE *et al.* 2008; KULKARNI *et al.* 2009; HOU *et al.* 2012),

510   whereas non-cancerous cells arrest in G1 and resume proliferation after Cdc7 activity is restored

511   (RODRIGUEZ-ACEBES *et al.* 2010). Currently, Cdc7 inhibitors are in clinical trials to

512   downregulate Cdc7 activity in cancer cells (clinicaltrials.gov #'s NCT02699749,

513   NCT03096054). The evolutionary conservation of CENP-A and DDK makes budding yeast an

514   excellent model to investigate the molecular role of DDK in preventing mislocalization of

515   CENP-A and CIN.

TABLE

Table 1. Twelve mutant alleles with the lowest score from a Synthetic Genetic Array (SGA) with temperature sensitive gene mutants overexpressing *CSE4*. Listed are the top twelve conditional alleles of essential genes that displayed SDL when *CSE4* is expressed from a galactose-inducible promoter (AU *et al.* 2020). Shown are the mutant allele, SGA score as the epsilon value calculated as previously in (COSTANZO *et al.* 2010; COSTANZO *et al.* 2016) with a negative value indicating a defect in growth, human orthologue (https://yeastmine.yeastgenome.org/yeastmine), and gene ontology (GO) annotation (https://www.yeastgenome.org/).

	Mutant	SGA score	Human orthologue	GO Category
1	*cdc7-4*	-1.348	*CDC7*	DNA-dependent DNA replication initiation
2	*dbf4-2*	-1.22	*DBF4*	DNA-dependent DNA replication initiation
3	*dbf4-ts*	-1.206	*DBF4*	DNA-dependent DNA replication initiation
4	*gpi12-ph*	-1.13	*PIGL*	GPI anchor biosynthetic process
5	*cdc23-1*	-1.113	*CDC23*	Regulation of mitotic metaphase/anaphase transition
6	*cmd1-1*	-1.031	*CALML3/5*	Phosphatidylinositol biosynthetic process
7	*dbf4-1*	-0.989	*DBF4*	DNA-dependent DNA replication initiation
8	*sts1-ph*	-0.975		Proteasome localization
9	*hrp1-1*	-0.94	*HNRNPA2B1*	mRNA polyadenylation
10	*rna15-58*	-0.937		mRNA polyadenylation
11	*cdc7-1*	-0.927	*CDC7*	DNA-dependent DNA replication initiation
12	*pre2-75*	-0.916	*PSMB11*	Proteasome core complex assembly

540

FIGURES LEGENDS

542 **Figure 1. DDK mutants exhibit synthetic dosage lethality (SDL) to *GALCSE4*. A.**

543 **Validation of *GALCSE4* SDL in *cdc7* and *dbf4* strains.** Growth assays were done with wild

544 type [BY4741 (for *cdc7-4*, *dbf4-1*, and *dbf4-2*) and RSY299 (for *cdc7-7*)], *cdc7-4* (tsa131), *dbf4-*

545 *1* (tsa161), *dbf4-2* (tsa162), and *cdc7-7* (RSY302) strains transformed with vector (pMB433,

546 vector) or *GAL-HA-CSE4* (SB878, *GALCSE4*). Cells were spotted in five-fold serial dilutions on

547 medium selective for the plasmid containing either glucose (2%, Cse4 expression off) or

548 raffinose/galactose (2% each, Cse4 expression is on) and incubated at 23°C for 3-5 days. Two

549 independent transformants of *dbf4-1*, *dbf4-2*, and *cdc7-4* strains and three independent

550 transformants of *cdc7-7* strains were assayed and a representative image is shown. **B. The**

551 ***GALCSE4* SDL phenotype of a *cdc7-7* strain is linked to the *cdc7* mutant allele.** Growth

552 assays were done with *cdc7-7* strains (RSY302 with pMB433 and RSY302 with pMB1597)

553 transformed with empty vector (pRS425) or plasmid-born *CDC7* (pMB1898). Cells were spotted

554 in five-fold serial dilutions on medium selective for the plasmids with glucose (2%) or

555 raffinose/galactose (2% each). Plates were incubated at the indicated temperature for 5-7 days.

556 Three independent transformants for each strain were assayed and a representative image is

557 shown.

558

559 **Figure 2. Cdc7 regulates ubiquitin-mediated proteolysis of Cse4. A. Cse4 is stabilized in a**

560 ***cdc7* strain** and **B. Cse4 is stabilized in a *dbf4* strain.** Western blot analysis of protein extracts

561 prepared from wild type (BY471 for *dbf4-1* and RSY299 for *cdc7-7*), (**A**) *cdc7-7* (RSY302), and

562 (**B**) *dbf4-1* (TSA161) strains transformed with *GAL-HA-CSE4* (pMB1597). Strains were grown

563 to logarithmic phase of growth in raffinose-containing media (2%), and expression of *GAL-HA-*

564   *CSE4* was induced with galactose (2%) for four hours. Cells were then treated with

565   cycloheximide (CHX, 10 µg/ml) and glucose (2%). Aliquots were taken at the indicated

566   timepoints. Protein extracts were analyzed using Western blot analysis and blots were probed

567   with anti-HA (Cse4) and anti-Tub2. (loading control). Quantification of the levels of HA-Cse4

568   remaining after treatment with CHX relative to Tub2 from two independent experiments is

569   shown in the graphs. Error bars represent SEM. **C. Ubiquitination of Cse4 is decreased in a**

570   ***cdc7* strain.** Ub-pull down assays were performed using protein extracts from wild type and

571   *cdc7-7* strains as described above and lysates were incubated with Tandem Ubiquitin Binding

572   Entity beads (LifeSensors). Input and ubiquitin-enriched (Pull down: Ub^+) samples were

573   analyzed via Western blot against HA (left). Arrow indicates the unmodified Cse4 band.

574   Quantification of levels of poly-ubiquitinated Cse4 (Ub_n-Cse4) normalized to the levels in the

575   input from three independent experiments is shown in the graph, *p*-value < 0.05.

576

577   **Figure 3. Cdc7 regulates stability of Cse4 independently of its role in initiation of DNA**

578   **replication. A. A *cdc7-7 mcm5-bob1* strain shows SDL with *GALCSE4*.** Growth assays with

579   wild type (RSY299), *mcm5-bob1* (RSY867), *cdc7-7* (RSY302), or *cdc7-7 mcm5-bob1* (RSY847)

580   strains transformed with vector (pMB433, vector) or *GAL-HA-CSE4* (SB878, *GALCSE4*). Cells

581   were spotted in five-fold serial dilutions on media selective for the plasmid containing either

582   glucose (2%) or raffinose/galactose (2% each) and incubated at 23°C for 3-5 days. Three

583   independent transformants for each strain were assayed and the representative image is shown.

584   **B. A *cdc7-7 mcm5-bob1* strain exhibits defects in Cse4 proteolysis.** Western blot analysis of

585   protein extracts from wild type (RSY299), *mcm5-bob1* (RSY867), *cdc7-7* (RSY302), or *cdc7-7*

586   *mcm5-bob1* (RSY847) strains transformed with *GAL-HA-CSE4* (pMB1597). Strains were grown

587   to logarithmic phase of growth in raffinose-containing media (2%) and expression of *GAL-HA-*

588   *CSE4* was induced with galactose (2%) for four hours. Cells were then treated with

589   cycloheximide (CHX, 10 µg/ml) and glucose (2%). Aliquots were taken at the indicated

590   timepoints. Protein extracts were analyzed using Western blot analysis and blots were probed

591   with anti-HA (Cse4) and anti-Tub2. (loading control). The graph shows the quantification of

592   levels of HA-Cse4 remaining after treatment with CHX relative to Tub2 from two independent

593   experiments. Error bars represent SEM.

594

595   **Figure 4. Cdc7 prevents mislocalization of Cse4 to non-centromeric regions. A. Cse4 is**

596   **mislocalized in a *cdc7* strain.** Localization of Cse4 was examined using chromosome spreads

597   prepared from nocodazole arrested wild type (RSY299) and *cdc7-7* (RSY302) strains

598   transformed with *GAL-HA-CSE4* (pMB1597). HA-Cse4 was labeled with Cy3 (red) and DNA

599   with DAPI (blue). Representative images of cells showing normal localization counted as nuclei

600   with one or two Cse4 foci (WT) and mislocalization counted as nuclei with more than two foci

601   or a diffuse signal in the nucleus (*cdc7-7*). Arrow indicates HA-Cse4 foci. **B. Quantification of**

602   **Cse4 localization from A.** The graph displays the quantification of Cse4 localization as a

603   percentage over total cell count. The SEM of two independent experiments is shown, WT 1 or 2

604   foci vs *cdc7-7* 1 or 2 Foci *p*-value = 0.0028; WT 3+ foci vs *cdc7-7* 3+ Foci *p*-value = 0.0028. **C.**

605   **The kinetochore protein Mtw1 is not mislocalized in a *cdc7-7* strain.** Wild type (YMB9337)

606   and *cdc7-7* (YMB9338) cells were transformed with Mtw1-GFP on a plasmid (pMB1058),

607   grown to logarithmic phase of growth, and analyzed for Mtw1-GFP (green) foci with live cell

608   imaging. Representative images of cells showing single Mtw1-GFP foci are shown. Arrow

609   indicates Mtw1-GFP foci. **D. Quantification of Mtw1-GFP localization from C.** The graph

610   displays the quantification of cells with one or two GFP foci (normal) or with greater than three

611   foci (mislocalized) with the SEM of two independent experiments; WT 1 or 2 foci vs *cdc7-7* 1 or

612   2 Foci *p*-value = 0.1683; WT 3+ foci vs *cdc7-7* 3+ Foci *p*-value = 0.1683.

613

614   **Figure 5. Cse4 is mislocalized to non-centromeric regions in a *cdc7-7* strain.** ChIP-seq was

615   performed using chromatin lysates from wild type (YMB10044) and *cdc7-7* (YMB10041)

616   strains. **A. Flag-Cse4 is mislocalized in a *cdc7-7* strain.** Genome browser of input and ChIP

617   samples for Chromosome I and Chromosome V in wild type (top) and *cdc7-7* (bottom) strains

618   overexpressing Flag-Cse4. Regions of *CEN1* and *CEN5* are shown. **B. Flag-Cse4 is enriched at**

619   **promoters in a *cdc7-7* strain.** The annotatePeaks tool of HOMER v5.10

620   (http://homer.ucsd.edu/homer/) was used to define genomic locations of Flag-Cse4 enrichment in

621   the *cdc7-7* strain. The genomic feature, peak number, percent of total peaks, region size, fold-

622   enrichment (relative to sequence content), and LogP enrichment are indicated. **C. FLAG-Cse4 is**

623   **preferentially enriched at promoters in *cdc7-7* and *psh1Δ* strains.** Overlap between Flag-

624   Cse4 enrichment in *cdc7-7* and *psh1Δ* strains and at promoters.

625

626   **Figure 6. Cdc7 regulates Psh1-mediated proteolysis of Cse4. A. Overexpression of *UBI4***

627   **suppresses the SDL of a *cdc7-7 GALCSE4* strain.** Growth assays of wild type (RSY299) and

628   *cdc7-7* (RSY302) cells transformed with empty vector (pMB433, *GALCSE4* -) or *GAL-HA-CSE4*

629   (pMB1597, *GALCSE4+*) and subsequently transformed with empty (pRS425, 2μ *UBI4-*) or

630   UBI4 (pMB1604, *UBI4+*). Cells were spotted in five-fold serial dilutions on media selective for

631   the plasmids containing either glucose (2%) or raffinose/galactose (2% each) and incubated at

632   23°C or 37°C as indicated for 3-5 days. Three independent transformants for each strain were

633 assayed and the representative image is shown. **B. The *GALCSE4* SDL phenotype of the *cdc7-***

634 ***7 psh1Δ* strain is similar to that observed for *psh1Δ* and *cdc7-7* strains.** Growth assays of

635 wild type, *psh1Δ*, *cdc7-7*, and *cdc7-7 psh1Δ* strains with endogenously expressed Flag-Cse4

636 (vector; YMB10043, YMB10126, YMB10040, and YMB10124, respectively) or Flag-Cse4

637 expressed from a galactose-inducible promoter integrated into the genome (*GALCSE4;*

638 YMB10044, YMB10127, YMB10041, and YMB10125, respectively) spotted in five-fold serial

639 dilutions on to rich media containing either glucose (2%) or raffinose/galactose (2% each) and

640 incubated at 23°C for 5 days. Three independent transformants for each strain were assayed and

641 the representative image is shown. **C. The Cse4 proteolysis defect in a *cdc7-7 psh1Δ* double**

642 **mutant is similar to that observed for a *psh1Δ* strain.** Western blot analysis of protein extracts

643 from wild type (YMB10044), *cdc7-7* (YMB10041), *psh1Δ* (YMB10127), and *cdc7-7 psh1Δ*

644 (YMB10125) strains grown to logarithmic phase of growth in raffinose-containing media (2%).

645 Expression of *GAL-FLAG-CSE4* was induced with galactose (2%) for 1.75 hours. Cells were

646 then treated with cycloheximide (CHX, 10 µg/ml) and glucose (2%). Aliquots were taken at the

647 indicated timepoints. Protein extracts were analyzed using Western blot analysis and blots were

648 probed with anti-FLAG (Cse4) and anti-Tub2. (loading control). The graph shows the

649 quantification of the levels of FLAG-Cse4 remaining after treatment with CHX relative to Tub2

650 from two independent experiments. Error bars represent SEM. **D. Mislocalization of Cse4 is not**

651 **further enhanced in the *cdc7-7 psh1Δ* strain.** Localization of Cse4 was examined using

652 chromosome spreads prepared from nocodazole arrested wild type (YMB10044), *cdc7-7*

653 (YMB10041), *psh1Δ* (YMB10127), and *cdc7-7 psh1Δ* (YMB10125). FLAG-Cse4 was labeled

654 with Cy3 and DNA with DAPI. The graph displays quantification of Cse4 localization as a

655 percentage over total cell count. The graph displays the SEM of two independent experiments,

656   *psh1Δ* 3+ foci vs *cdc7-7* 3+ Foci, *cdc7-7* 3+ foci vs *cdc7-7 psh1Δ* 3+ Foci, and *psh1Δ* 3+ foci vs

657   *cdc7-7 psh1Δ* 3+ Foci *p*-value > 0.999.

658
659 CITATIONS

660 Allshire, R. C., and G. H. Karpen, 2008 Epigenetic regulation of centromeric chromatin: old

661   dogs, new tricks? Nat Rev Genet 9**:** 923-937.

662 Amato, A., T. Schillaci, L. Lentini and A. Di Leonardo, 2009 CENPA overexpression promotes

663   genome instability in pRb-depleted human cells. Mol Cancer 8**:** 119.

664 Athwal, R. K., M. P. Walkiewicz, S. Baek, S. Fu, M. Bui *et al.*, 2015 CENP-A nucleosomes

665   localize to transcription factor hotspots and subtelomeric sites in human cancer cells.

666   Epigenetics Chromatin 8**:** 2.

667 Au, W. C., M. J. Crisp, S. Z. DeLuca, O. J. Rando and M. A. Basrai, 2008 Altered dosage and

668   mislocalization of histone H3 and Cse4p lead to chromosome loss in Saccharomyces

669   cerevisiae. Genetics 179**:** 263-275.

670 Au, W. C., A. R. Dawson, D. W. Rawson, S. B. Taylor, R. E. Baker *et al.*, 2013 A Novel Role of

671   the N-Terminus of Budding Yeast Histone H3 Variant Cse4 in Ubiquitin-Mediated

672   Proteolysis. Genetics 194**:** 513-518.

673 Au, W. C., T. Zhang, P. K. Mishra, J. R. Eisenstatt, R. L. Walker *et al.*, 2020 Skp, Cullin, F-box

674   (SCF)-Met30 and SCF-Cdc4-Mediated Proteolysis of CENP-A Prevents Mislocalization

675   of CENP-A for Chromosomal Stability in Budding Yeast. PLoS Genet 16**:** e1008597.

676 Baker, S. P., J. Phillips, S. Anderson, Q. Qiu, J. Shabanowitz *et al.*, 2010 Histone H3 Thr 45

677   phosphorylation is a replication-associated post-translational modification in S.

678   cerevisiae. Nat Cell Biol 12**:** 294-298.

679 Baryshnikova, A., M. Costanzo, S. Dixon, F. J. Vizeacoumar, C. L. Myers *et al.*, 2010 Synthetic

680   genetic array (SGA) analysis in Saccharomyces cerevisiae and Schizosaccharomyces

681   pombe. Methods Enzymol 470**:** 145-179.

682   Biggins, S., 2013 The Composition, Functions, and Regulation of the Budding Yeast

683   Kinetochore. Genetics 194**:** 817-846.

684   Boeckmann, L., Y. Takahashi, W. C. Au, P. K. Mishra, J. S. Choy *et al.*, 2013 Phosphorylation

685   of centromeric histone H3 variant regulates chromosome segregation in Saccharomyces

686   cerevisiae. Mol Biol Cell 24**:** 2034-2044.

687   Bonte, D., C. Lindvall, H. Liu, K. Dykema, K. Furge *et al.*, 2008 Cdc7-Dbf4 Kinase

688   Overexpression in Multiple Cancers and Tumor Cell Lines Is Correlated with p53

689   Inactivation. Neoplasia 10**:** 920-931.

690   Bruck, I., and D. Kaplan, 2009 Dbf4-Cdc7 Phosphorylation of Mcm2 is Required for Cell

691   Growth. J Biol Chem 284**:** 28823-28831.

692   Burrack, L. S., and J. Berman, 2012 Flexibility of centromere and kinetochore structures. Trends

693   Genet 28**:** 204-212.

694   Camahort, R., M. Shivaraju, M. Mattingly, B. Li, S. Nakanishi *et al.*, 2009 Cse4 is part of an

695   octameric nucleosome in budding yeast. Mol Cell 35**:** 794-805.

696   Cheng, A. N., S. S. Jiang, C. C. Fan, Y. K. Lo, C. Y. Kuo *et al.*, 2013 Increased Cdc7 expression

697   is a marker of oral squamous cell carcinoma and overexpression of Cdc7 contributes to

698   the resistance to DNA-damaging agents. Cancer Lett 337**:** 218-225.

699   Cheng, H., X. Bao, X. Gan, S. Luo and H. Rao, 2017 Multiple E3s promote the degradation of

700   histone H3 variant Cse4. Sci Rep 7**:** 8565.

701   Cheng, H., X. Bao and H. Rao, 2016 The F-box Protein Rcy1 Is Involved in the Degradation of

702   Histone H3 Variant Cse4 and Genome Maintenance. J Biol Chem 291**:** 10372-10377.

703   Chereji, R. V., J. Ocampo and D. J. Clark, 2017 MNase-Sensitive Complexes in Yeast:

704   Nucleosomes and Non-histone Barriers. Mol Cell 65**:** 565-577 e563.

705 Choy, J. S., P. K. Mishra, W. C. Au and M. A. Basrai, 2012 Insights into assembly and

706   regulation of centromeric chromatin in Saccharomyces cerevisiae. Biochim Biophys Acta

707   1819**:** 776-783.

708 Ciftci-Yilmaz, S., W. C. Au, P. K. Mishra, J. R. Eisenstatt, J. Chang *et al.*, 2018 A Genome-

709   Wide Screen Reveals a Role for the HIR Histone Chaperone Complex in Preventing

710   Mislocalization of Budding Yeast CENP-A. Genetics 210**:** 203-218.

711 Cole, H. A., J. Ocampo, J. R. Iben, R. V. Chereji and D. J. Clark, 2014 Heavy transcription of

712   yeast genes correlates with differential loss of histone H2B relative to H4 and queued

713   RNA polymerases. Nucleic Acids Res 42**:** 12512-12522.

714 Collins, K. A., R. Camahort, C. Seidel, J. L. Gerton and S. Biggins, 2007 The overexpression of

715   a Saccharomyces cerevisiae centromeric histone H3 variant mutant protein leads to a

716   defect in kinetochore biorientation. Genetics 175**:** 513-525.

717 Collins, K. A., S. Furuyama and S. Biggins, 2004 Proteolysis contributes to the exclusive

718   centromere localization of the yeast Cse4/CENP-A histone H3 variant. Curr Biol 14**:**

719   1968-1972.

720 Costanzo, M., A. Baryshnikova, J. Bellay, Y. Kim, E. D. Spear *et al.*, 2010 The genetic

721   landscape of a cell. Science 327**:** 425-431.

722 Costanzo, M., B. VanderSluis, E. N. Koch, A. Baryshnikova, C. Pons *et al.*, 2016 A global

723   genetic interaction network maps a wiring diagram of cellular function. Science 353.

724 Crotti, L. B., and M. A. Basrai, 2004 Functional roles for evolutionarily conserved Spt4p at

725   centromeres and heterochromatin in Saccharomyces cerevisiae. EMBO J 23**:** 1804-1814.

726 Deyter, G. M., and S. Biggins, 2014 The FACT complex interacts with the E3 ubiquitin ligase

727   Psh1 to prevent ectopic localization of CENP-A. Genes Dev 28**:** 1815-1826.

728   Fischböck-Halwachs, J., S. Singh, M. Potocnjak, G. Hagemann, V. Solis-Mezarino *et al.*, 2019

729   The COMA complex interacts with Cse4 and positions Sli15/Ipl1 at the budding yeast

730   inner kinetochore. eLife 8.

731   Gonzalez, M., H. He, Q. Dong, S. Sun and F. Li, 2014 Ectopic centromere nucleation by CENP--

732   a in fission yeast. Genetics 198**:** 1433-1446.

733   Hardy, C. F. J., O. Dryga, S. Seematter, P. M. B. Pahl and R. A. Sclafani, 1997 *mcm5/cdc46-*

734   *bob1* bypasses the requirement for the S phase activator Cdc7p. Proc. Natl. Acad. Sci.

735   USA 94**:** 3151-3155.

736   Henikoff, S., and T. Furuyama, 2012 The unconventional structure of centromeric nucleosomes.

737   Chromosoma 121**:** 341-352.

738   Heun, P., S. Erhardt, M. D. Blower, S. Weiss, A. D. Skora *et al.*, 2006 Mislocalization of the

739   Drosophila centromere-specific histone CID promotes formation of functional ectopic

740   kinetochores. Dev Cell 10**:** 303-315.

741   Hewawasam, G., M. Shivaraju, M. Mattingly, S. Venkatesh, S. Martin-Brown *et al.*, 2010 Psh1

742   is an E3 ubiquitin ligase that targets the centromeric histone variant Cse4. Mol Cell 40**:**

743   444-454.

744   Hewawasam, G. S., M. Mattingly, S. Venkatesh, Y. Zhang, L. Florens *et al.*, 2014

745   Phosphorylation by casein kinase 2 facilitates Psh1 protein-assisted degradation of Cse4

746   protein. J Biol Chem 289**:** 29297-29309.

747   Hildebrand, E. M., and S. Biggins, 2016 Regulation of Budding Yeast CENP-A levels Prevents

748   Misincorporation at Promoter Nucleosomes and Transcriptional Defects. PLoS Genet 12**:**

749   e1005930.

750 Hinshaw, S. M., and S. C. Harrison, 2019 The structure of the Ctf19c/CCAN from budding

751   yeast. eLife 8.

752 Hinshaw, S. M., V. Makrantoni, S. C. Harrison and A. l. Marston, 2017 The Kinetochore

753   Receptor for the Cohesin Loading Complex. Cell 171**:** 72-84.

754 Hoang, M. L., R. P. Leon, L. Pessoa-Brandao, S. Hunt, M. K. Raghuraman *et al.*, 2007 Structural

755   changes in Mcm5 protein bypass Cdc7-Dbf4 function and reduce replication origin

756   efficiency in Saccharomyces cerevisiae. Mol Cell Biol 27**:** 7594-7602.

757 Hollingsworth Jr, R. E., R. M. Ostroff, M. B. Klein, L. A. Niswander and R. A. Sclafani, 1992

758   Molecular Genetic Studies of the Cdc7 Protein Kinase and Induced Mutagenesis in

759   Yeast. Genetics 132**:** 53-62.

760 Hou, Y., H. Q. Wang and Y. Ba, 2012 High expression of cell division cycle 7 protein correlates

761   with poor prognosis in patients with diffuse large B-cell lymphoma. Med Oncol 29**:**

762   3498-3503.

763 Jackson, A. L., P. M. B. Pahl, K. Harrison, J. Rosamond and R. A. Sclafani, 1993 Cell Cycle

764   Regulation of the Yeast Cdc7 Protein Kinase by

765 Association with the Dbf4 Proteint. Molecular and Cellular Biology 13**:** 2899-2908.

766 Kastenmayer, J. P., L. Ni, A. Chu, L. E. Kitchen, W. C. Au *et al.*, 2006 Functional genomics of

767   genes with small open reading frames (sORFs) in S. cerevisiae. Genome Res 16**:** 365-

768   373.

769 Kulkarni, A. A., S. R. Kingsbury, S. Tudzarova, H. K. Hong, M. Loddo *et al.*, 2009 Cdc7 kinase

770   is a predictor of survival and a novel therapeutic target in epithelial ovarian carcinoma.

771   Clin Cancer Res 15**:** 2417-2425.

772 Lacoste, N., A. Woolfe, H. Tachiwana, A. V. Garea, T. Barth *et al.*, 2014 Mislocalization of the

773   centromeric histone variant CenH3/CENP-A in human cells depends on the chaperone

774   DAXX. Mol Cell 53**:** 631-644.

775 Lefrancois, P., G. M. Euskirchen, R. K. Auerbach, J. Rozowsky, T. Gibson *et al.*, 2009 Efficient

776   yeast ChIP-Seq using multiplex short-read DNA sequencing. BMC Genomics 10.

777 Lei, M., Y. Kawasaki, M. R. Young, M. Kihara, A. Sugino *et al.*, 1997 Mcm2 is a target of

778   regulation by Cdc7-Dbf4 during the initiation of DNA synthesis. Genes Dev 11**:** 3365-

779   3374.

780 Li, Y., Z. Zhu, S. Zhang, D. Yu, H. Yu *et al.*, 2011 ShRNA-targeted centromere protein A

781   inhibits hepatocellular carcinoma growth. PLoS One 6**:** e17794.

782 Maddox, P. S., K. D. Corbett and A. Desai, 2012 Structure, assembly and reading of centromeric

783   chromatin. Curr Opin Genet Dev 22**:** 139-147.

784 McGovern, S. L., Y. Qi, L. Pusztai, W. F. Symmans and T. A. Buchholz, 2012 Centromere

785   protein-A, an essential centromere protein, is a prognostic marker for relapse in estrogen

786   receptor-positive breast cancer. Breast Cancer Res 14**:** R72.

787 McKinley, K. L., and I. M. Cheeseman, 2016 The molecular basis for centromere identity and

788   function. Nat Rev Mol Cell Biol 17**:** 16-29.

789 Mishra, P. K., W. C. Au, J. S. Choy, P. H. Kuich, R. E. Baker *et al.*, 2011 Misregulation of

790   Scm3p/HJURP causes chromosome instability in Saccharomyces cerevisiae and human

791   cells. PLoS Genet 7**:** e1002303.

792 Montagnoli, A., P. Tenca, F. Sola, D. Carpani, D. Brotherton *et al.*, 2004 Cdc7 inhibition reveals

793   a p53-dependent replication checkpoint that is defective in cancer cells. Cancer Res 63**:**

794   7110-7116.

795   Moreno-Moreno, O., S. Medina-Giro, M. Torras-Llort and F. Azorin, 2011 The F box protein

796   partner of paired regulates stability of Drosophila centromeric histone H3, CenH3(CID).

797   Curr Biol 21**:** 1488-1493.

798   Moreno-Moreno, O., M. Torras-Llort and F. Azorin, 2006 Proteolysis restricts localization of

799   CID, the centromere-specific histone H3 variant of Drosophila, to centromeres. Nucleic

800   Acids Res 34**:** 6247-6255.

801   Nagalakshmi, U., Z. Wang, K. Waern, C. Shou, D. Raha *et al.*, 2008 The Transcriptional

802   Landscape of the Yeast Genome Defined by RNA Sequencing. Science 320**:** 1344-1349.

803   Natsume, T., C. A. Muller, Y. Katou, R. Retkute, M. Gierlinski *et al.*, 2013 Kinetochores

804   coordinate pericentromeric cohesion and early DNA replication by Cdc7-Dbf4 kinase

805   recruitment. Mol Cell 50**:** 661-674.

806   Ohkuni, K., R. Levy-Myers, J. Warren, W. C. Au, Y. Takahashi *et al.*, 2018 N-terminal

807   Sumoylation of Centromeric Histone H3 Variant Cse4 Regulates Its Proteolysis To

808   Prevent Mislocalization to Non-centromeric Chromatin. G3 (Bethesda) 8**:** 1215-1223.

809   Ohkuni, K., Y. Takahashi, A. Fulp, J. Lawrimore, W. C. Au *et al.*, 2016 SUMO-Targeted

810   Ubiquitin Ligase (STUbL) Slx5 regulates proteolysis of centromeric histone H3 variant

811   Cse4 and prevents its mislocalization to euchromatin. Mol Biol Cell.

812   Oshiro, G., J. C. Owens, Y. Shellman, R. A. Sclafani and J. J. Li, 1999 Cell cycle control of

813   Cdc7p kinase activity through regulation of Dbf4p stability. Mol Cell Biol 19**:** 4888-

814   4896.

815   Owens, J. C., C. S. Detweller and J. J. Li, 1997 CDC45 is required in conjunction with

816   CDC7/DBF4 to trigger the initiation of DNA replication. Proc Natl Acad Sci U S A 94**:**

817   12521-12526.

818   Pessoa-Brandao, L., and R. A. Sclafani, 2004 CDC7/DBF4 functions in the translesion synthesis

819   branch of the RAD6 epistasis group in Saccharomyces cerevisiae. Genetics 167**:** 1597-

820   1610.

821   Pinsky, B. A., S. Y. Tatsutani, K. A. Collins and S. Biggins, 2003 An Mtw1 complex promotes

822   kinetochore biorientation that is monitored by the Ipl1/Aurora protein kinase. Dev Cell 5**:**

823   735-745.

824   Przewloka, M. R., and D. M. Glover, 2009 The kinetochore and the centromere: a working long

825   distance relationship. Annu Rev Genet 43**:** 439-465.

826   Raghuraman, M. K., E. A. Winzeler, D. Collingwood, S. Hunt, L. Wodicka *et al.*, 2001

827   Replication Dynamics of the Yeast Genome. Science 294**:** 115-121.

828   Ranjitkar, P., M. O. Press, X. Yi, R. Baker, M. J. MacCoss *et al.*, 2010 An E3 ubiquitin ligase

829   prevents ectopic localization of the centromeric histone H3 variant via the centromere

830   targeting domain. Mol Cell 40**:** 455-464.

831   Robinson, J. T., H. Thorvaldsottir, W. Winckler, M. Guttman, E. S. Lander *et al.*, 2011

832   Integrative genomics viewer. Nat Biotechnol 29**:** 24-26.

833   Rodriguez-Acebes, S., I. Proctor, M. Loddo, A. Wollenschlaeger, M. Rashid *et al.*, 2010

834   Targeting DNA replication before it starts: Cdc7 as a therapeutic target in p53-mutant

835   breast cancers. Am J Pathol 177**:** 2034-2045.

836   Rossbach, D., D. S. Bryan, J. R. Hesselberth and R. Sclafani, 2017 Localization of Cdc7 Protein

837   Kinase During DNA Replication in Saccharomyces cerevisiae. G3 7**:** 3757-3774.

838   Rossbach, D., and R. A. Sclafani, 2016 CDC7/DBF4 functions in the translesion synthesis

839   branch of the RAD6 epistasis group in Saccharomyces cerevisiae, pp. 279-296 in *The*

840   *Initiation of DNA Replication in Eukaryotes*, edited by D. L. Kaplan. Springer

841   International Publishing, New York.

842   Sclafani, R. A., 2000 Cdc7p-Dbf4p becomes famous in the cell cycle. Journal of Cell Science

843   113**:** 2111-2117.

844   Sclafani, R. A., M. Tecklenburg and A. Pierce, 2002 The *mcm5-bob1* Bypass of Cdc7p/Dbf4p in

845   DNA Replication Depends on Both Cdk1-Independent and Cdk1-Dependent Steps in

846   Saccharomyces cerevisiae. Genetics 161**:** 47-57.

847   Shrestha, R. L., G. S. Ahn, M. I. Staples, K. M. Sathyan, T. S. Karpova *et al.*, 2017

848   Mislocalization of centromeric histone H3 variant CENP-A contributes to chromosomal

849   instability (CIN) in human cells. Oncotarget 8**:** 46781-46800.

850   Stillman, B., 1996 Cell Cycle Control of DNA Replication. Science 274**:** 1659-1663.

851   Sun, X., P. L. Clermont, W. Jiao, C. D. Helgason, P. W. Gout *et al.*, 2016 Elevated expression of

852   the centromere protein-A(CENP-A)-encoding gene as a prognostic and predictive

853   biomarker in human cancers. Int J Cancer 139**:** 899-907.

854   Tomonaga, T., K. Matsushita, S. Yamaguchi, T. Oohashi, H. Shimada *et al.*, 2003

855   Overexpression and mistargeting of centromere protein-A in human primary colorectal

856   cancer. Cancer Res 63**:** 3511-3516.

857   Verdaasdonk, J. S., and K. Bloom, 2011 Centromeres: unique chromatin structures that drive

858   chromosome segregation. Nat Rev Mol Cell Biol 12**:** 320-332.

859   Weinreich, M., and B. Stillman, 1999 Cdc7p-Dbf4p kinase binds to chromatin during S phase

860   and is regulated by both the APC and the RAD53 checkpoint pathway. EMBO J 18**:**

861   5334-5346.

862   Westermann, S., I. M. Cheeseman, S. Anderson, J. R. Yates, 3rd, D. G. Drubin *et al.*, 2003

863   Architecture of the budding yeast kinetochore reveals a conserved molecular core. J Cell

864   Biol 163**:** 215-222.

865   Wong, C. Y. Y., B. C. H. Lee and K. W. Y. Yuen, 2020 Epigenetic regulation of centromere

866   function. Cell Mol LIfe Sci.

867   Zhang, W., J. H. Mao, W. Zhu, A. K. Jain, K. Liu *et al.*, 2016 Centromere and kinetochore gene

868   misexpression predicts cancer patient survival and response to radiotherapy and

869   chemotherapy. Nat Commun 7**:** 12619.

870   Zhang, Y., T. Liu, C. A. Meyer, J. Eeckhoute, D. S. Johnson *et al.*, 2008 Model-based Analysis

871   of ChIP-Seq (MACS). Genome Biology 9**:** R137.

872   Zou, L., and B. Stillman, 2000 Assembly of a complex containing Cdc45p, replication protein A,

873   and Mcm2p at replication origins controlled by S-phase cyclin-dependent kinases and

874   Cdc7p-Dbf4p kinase. Mol Biol Cell 20**:** 3086-3096.
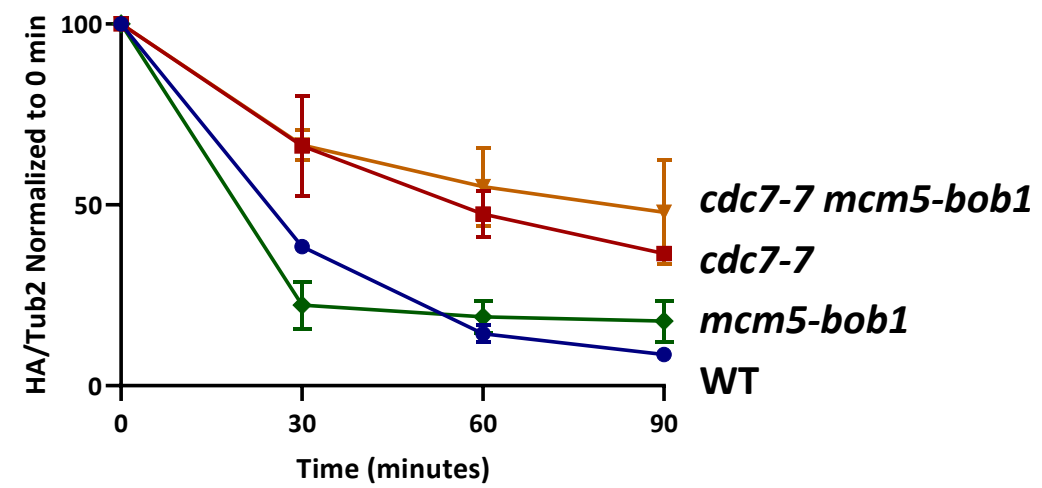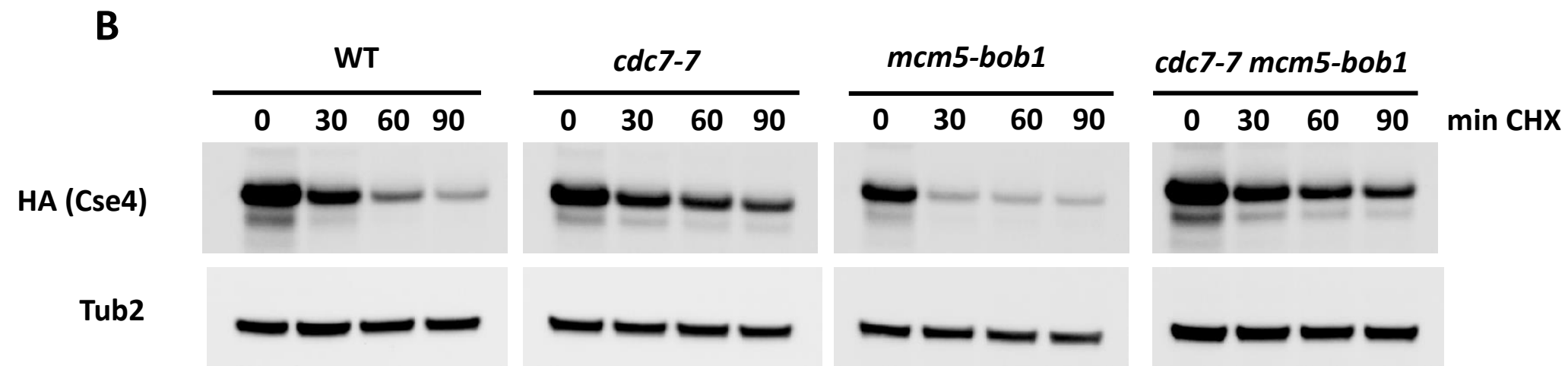
875

Figure 1

Figure 2

A

WT   cdc7-7

0 30 60 90 120   0 30 60 90 120 min CHX

HA (Cse4)

Tub2

B

WT   dbf4-1

0 30 60 90 120   0 30 60 90 120 min CHX

HA (Cse4)

Tub2

C

Input   Pull down: Ub$^+$

WT   cdc7-7   WT   cdc7-7

kDa

62 -

49 -

38-

Ub$_n$–Cse4

HA (Cse4)

$p < 0.05$

Relative Cse4-Ubiquitination

WT   cdc7-7

Figure 3

A
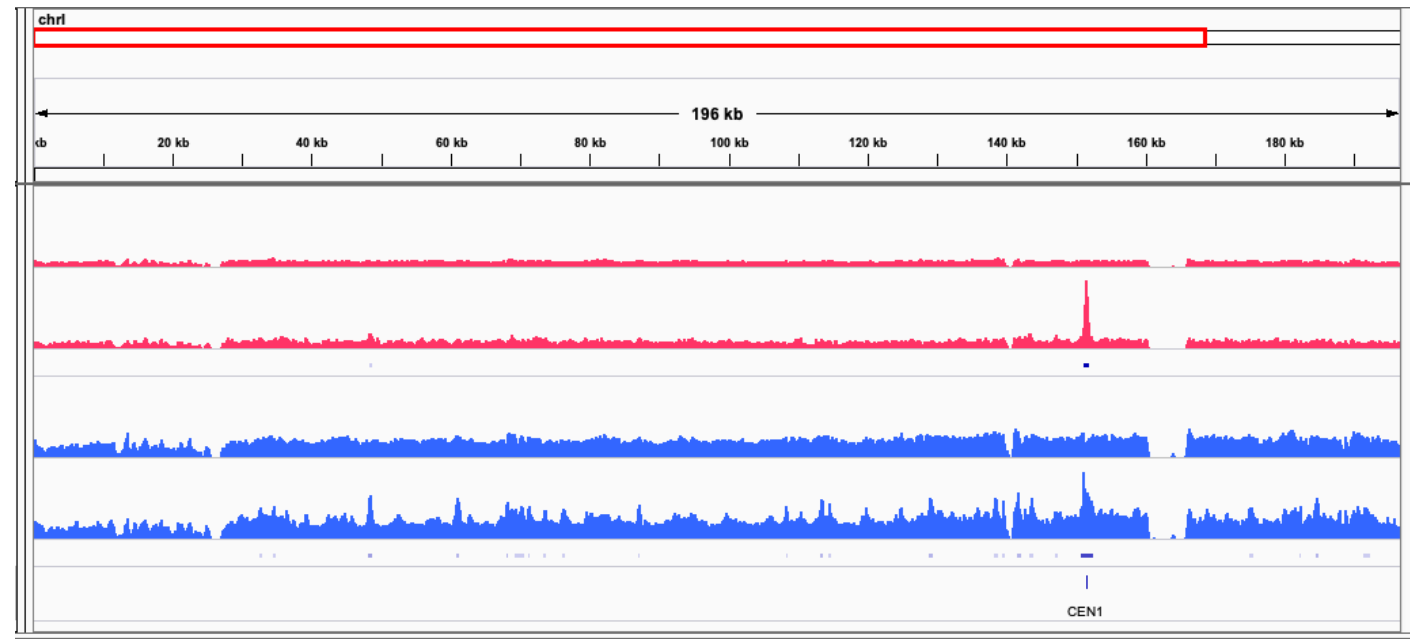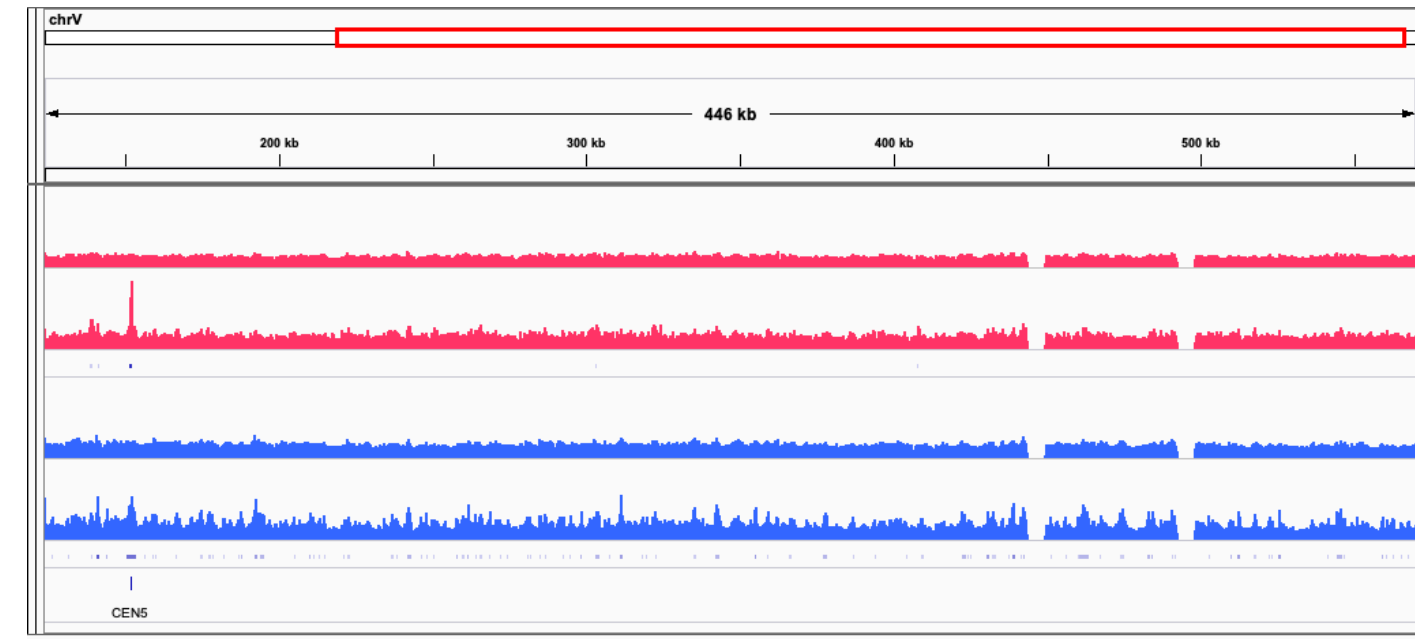
23°C

B
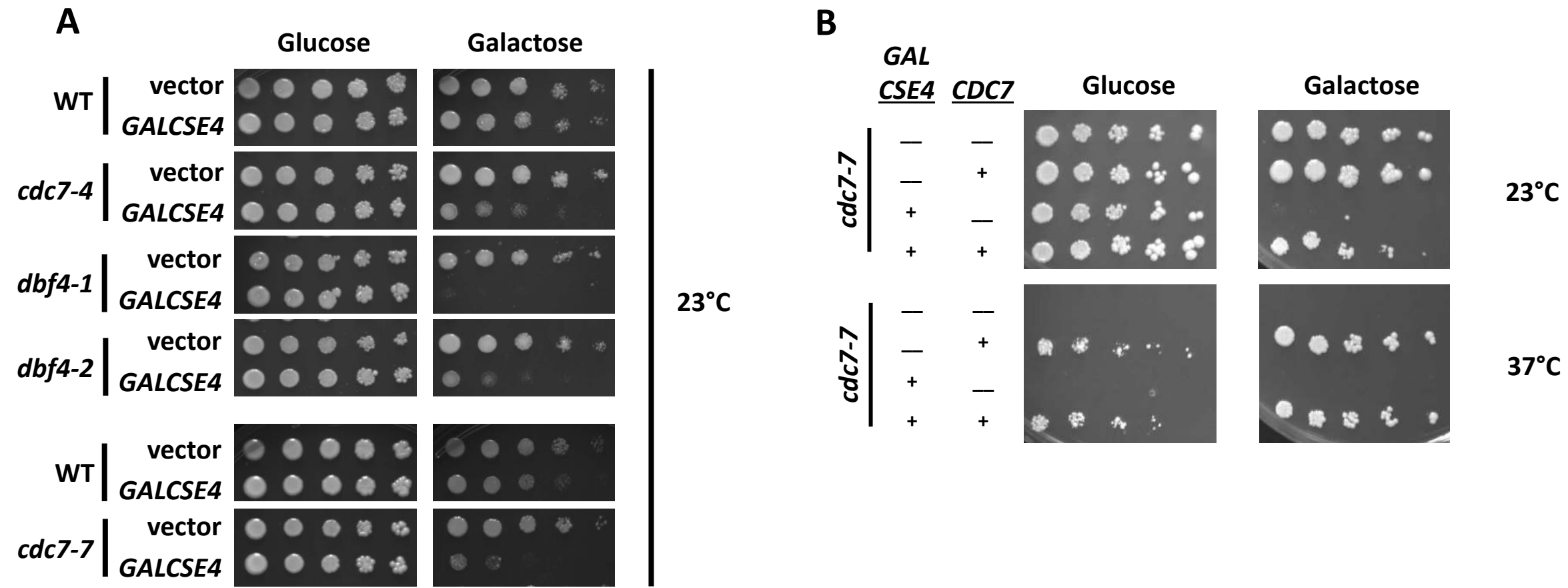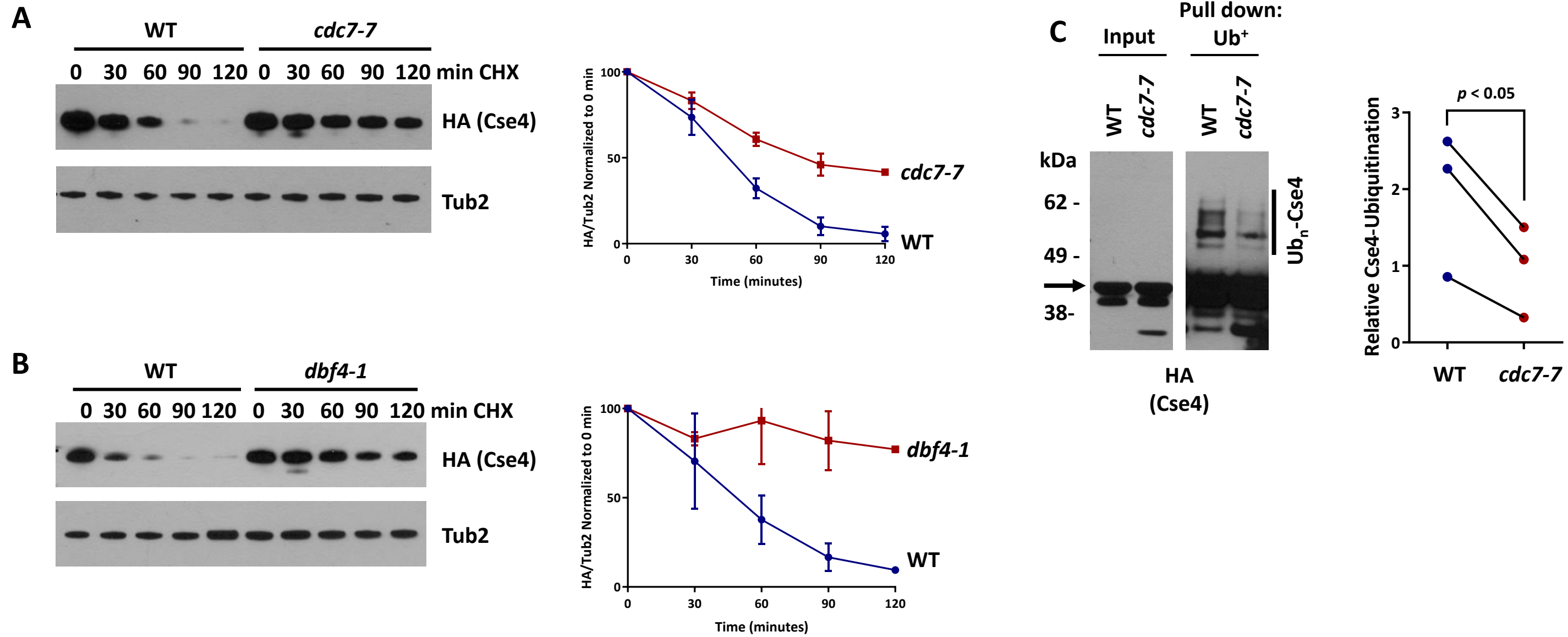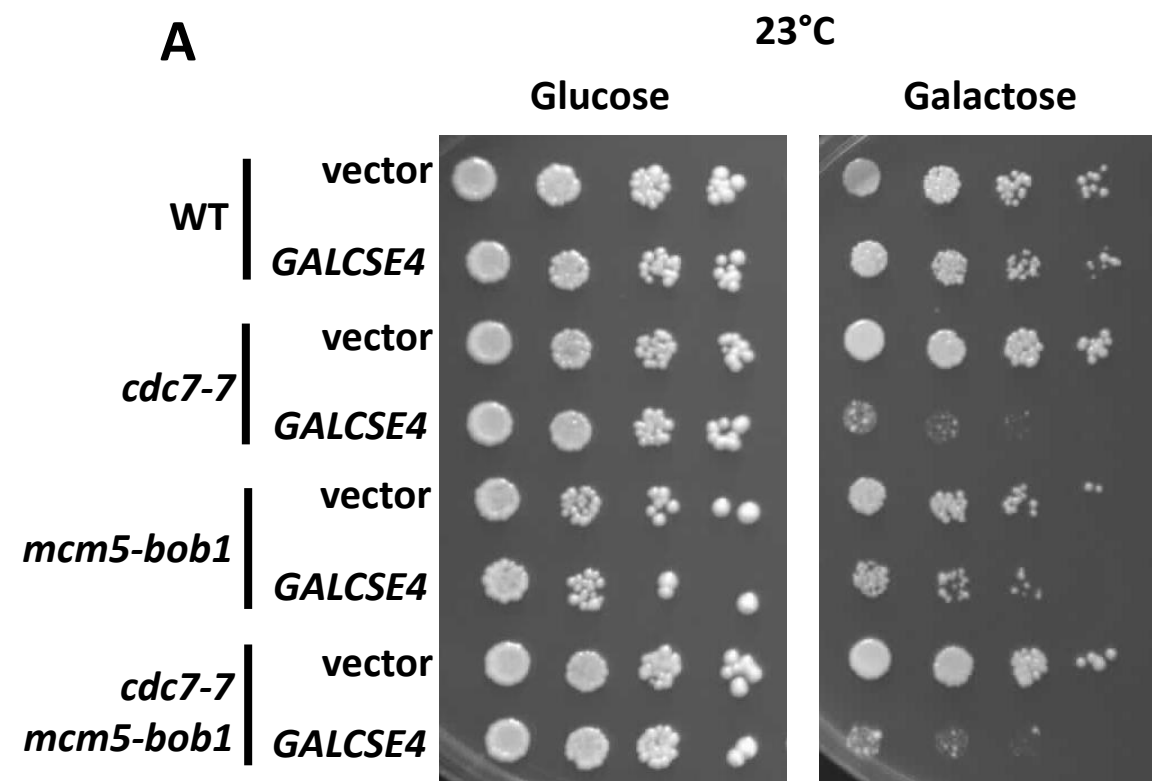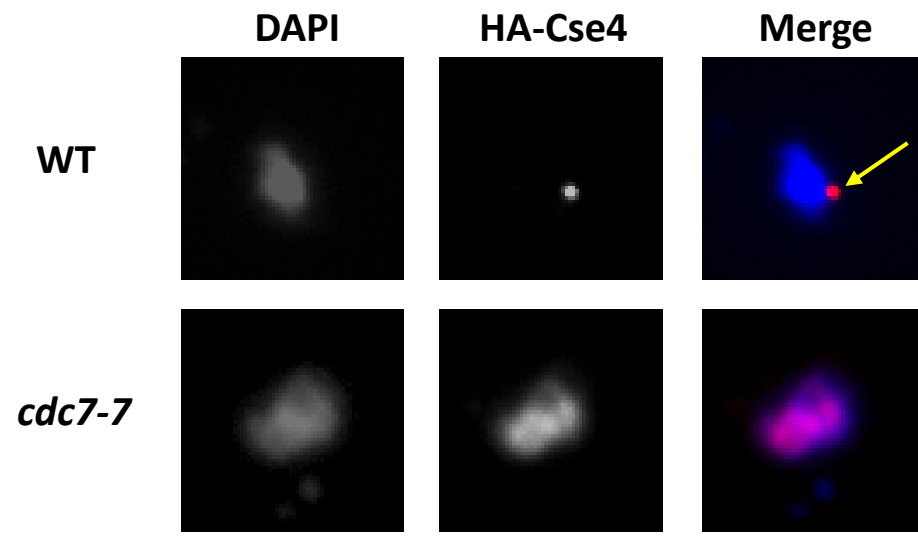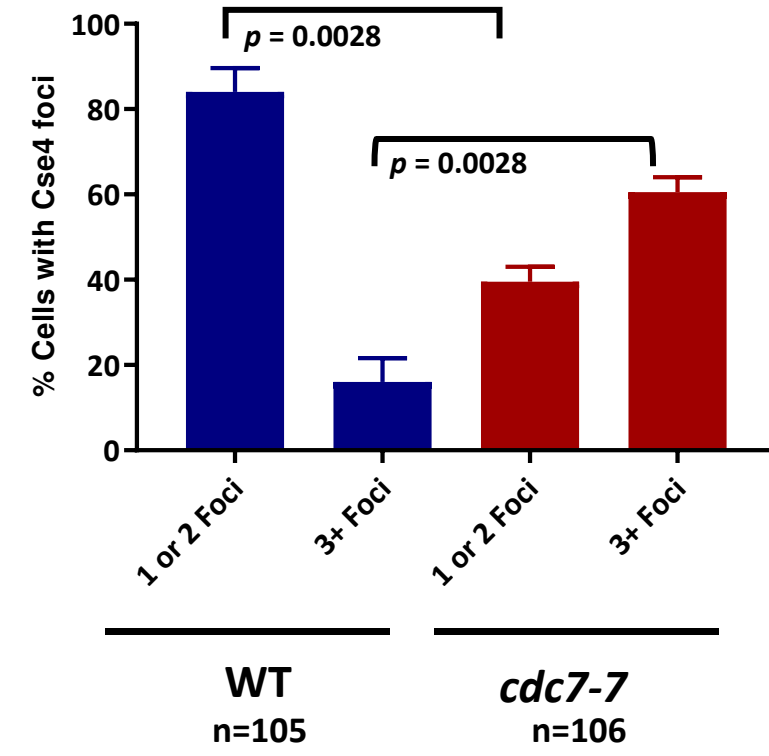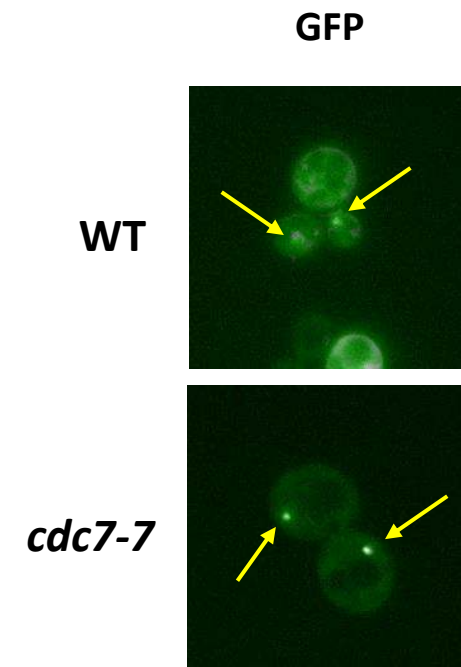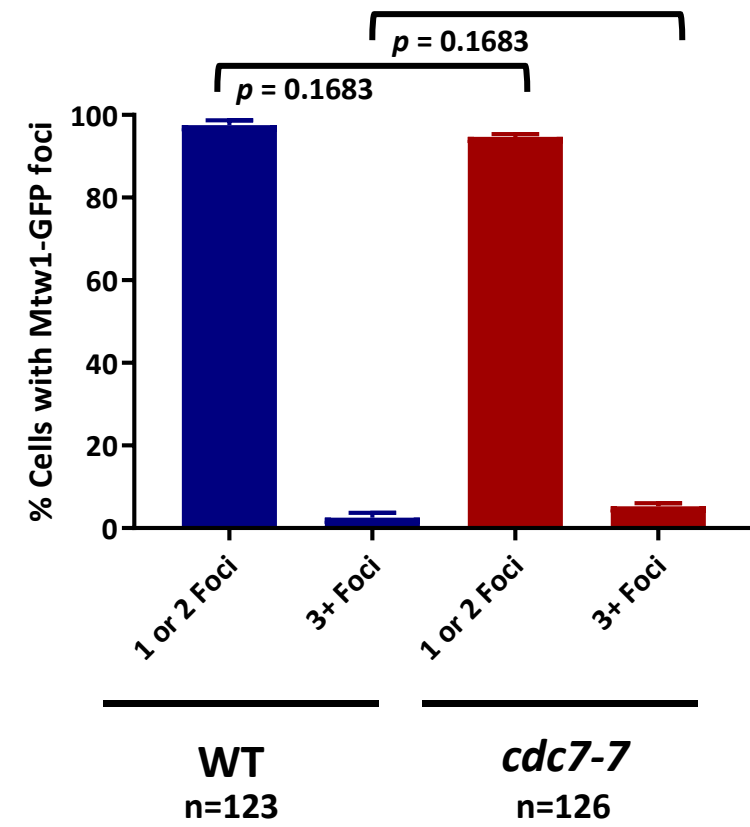
Figure 4

Figure 5

A

ChrI

ChrV

B

Peak Annotations in *cdc7-7 GALCSE4*	Number of Peaks	% of Total	Total Size (bp)	Enrichment (Obs/Exp)	LogP Enrichment (+values depleted)
3' UTR	28	1.3%	868412	0.2222	60.544
Transcription Termination Site	24	1.1%	666400	0.2481	42.749
Exons	457	20.7%	9031012	0.3487	694.356
Introns	12	0.5%	66236	1.2483	-1.347
Intergenic	136	6.2%	739256	1.2675	-5.667
Promoters	1330	60.4%	3330000	2.7511	-758.277
5' UTR	216	9.8%	476819	3.1210	-107.426
Total	2203		15178135		

C

psh1Δ (4798)

cdc7-7 (2129)

Promoters (4604)

816

99

1923

1960

36

34

687

Figure 6